**UNIVERSITY OF GAZİANTEP**
**GRADUATE SCHOOL OF**
**NATURAL & APPLIED SCIENCES**

**HIGH EARLY STRENGTH DUCTILE CEMENTITIOUS**
**COMPOSITES WITH CHARACTERISTICS OF LOW EARLY**
**AGE SHRINKAGE**

**M. Sc. THESIS**
**IN**
**CIVIL ENGINEERING**

**BY**
**YUNUS EMRE ŞİMŞEK**
**APRIL 2013**

**High Early Strength Ductile Cementitious Composites with Characteristics of Low Early Age Shrinkage**

**M.Sc. Thesis**
**in**
**Civil Engineering**
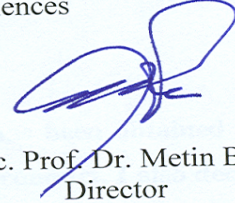**University of Gaziantep**

**Supervisor**
**Assoc. Prof. Dr. Mustafa ŞAHMARAN**

**by**
**Yunus Emre ŞİMŞEK**
**April 2013**

T.C.
UNIVERSITY OF GAZİANTEP
GRADUATE SCHOOL OF
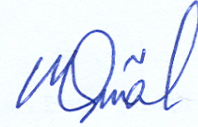NATURAL & APPLIED SCIENCES
CIVIL ENGINEERING DEPARTMENT

Name of the thesis: High Early Strength Ductile Cementitious Composites with Characteristics of Low Early Age Shrinkage
Name of the student: Yunus Emre ŞİMŞEK
Exam date: 24.04.2013

Approval of the Graduate School of Natural and Applied Sciences
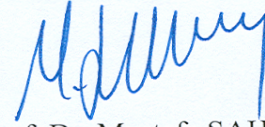
Assoc. Prof. Dr. Metin BEDİR
Director

I certify that this thesis satisfies all the requirements as a thesis for the degree of Master of Science.

Prof. Dr. Mustafa GÜNAL
Head of Department

This is to certify that we have read this thesis and that in our opinion it is fully adequate, in scope and quality, as a thesis for the degree of Master of Science.

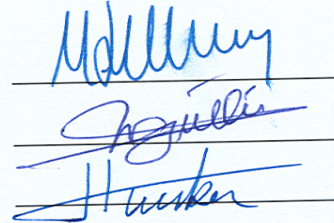Assoc. Prof. Dr. Mustafa ŞAHMARAN
Supervisor

Examining Committee Members                           Signature

Assoc. Prof. Dr. Mustafa ŞAHMARAN        _____

Asst. Prof. Dr. Hamza GÜLLÜ                    _____

Asst. Prof. Dr. Hakan Tacettin TÜRKER       _____

I hereby declare that all information in this document has been obtained and presented in accordance with academic rules and ethical conduct. I also declare that, as required by these rules and conduct, I have fully cited and referenced all material and results that are not original to this work.


Yunus Emre ŞİMŞEK

# ABSTRACT

## HIGH EARLY STRENGTH DUCTILE CEMENTITIOUS COMPOSITES WITH CHARACTERISTICS OF LOW EARLY AGE SHRINKAGE

ŞİMŞEK, Yunus Emre
M.Sc. in Civil Engineering
Supervisor: Assoc. Prof. Dr. Mustafa ŞAHMARAN
April 2013, 72 pages

Reduced performance in concrete infrastructures is mainly caused by the formation of cracks, which may arise due to deteriorating mechanisms during service life. In most cases, reduced performance calls for urgent repairs to the degraded section. Therefore, it is highly desirable to develop dimensionally stable, ductile repair materials that can attain adequately high strength in a limited amount of time, compensate for significant deformation due to mechanical and environmental loadings, and prevent early-age shrinkage cracks. In this paper, the performance of such a material (High Early Strength Engineered Cementitious Composites – HES-ECC with very low early-age shrinkage capacity) was investigated by studying mechanical properties and dimensional stability. Composites were produced with different water to cementitious materials and slag to Portland cement ratios. In order to rehabilitate composite properties in terms of ductility and early age shrinkage characteristics, saturated lightweight aggregates replaced sand in the mixtures. The experimental results show that the majority of HES-ECC mixtures developed in this study attained compressive strength values of more than 20.0 MPa and minimum flexural strength of 6.0 MPa within six hours. Moreover, the HES-ECC mixtures exhibited strain-hardening behavior with strain capacities comparable to normal strength ECC, as well as substantially reduced autogenous shrinkage strain capacity, both which are unlikely to trigger the formation of cracks in tension at early ages. The integration of these conflicting parameters suggests that HES-ECC can easily meet the need for fast and durable repairs.

**Keywords:** High-Early-Strength-Engineered Cementitious Composites (HES-ECC); Lightweight aggregates (LWA); Mechanical properties; Dimensional stability.

# ÖZET

## DÜŞÜK ERKEN YAŞ RÖTRE ÖZELLİĞİNE SAHİP ERKEN YÜKSEK DAYANIMLI SÜNEK ÇİMENTO BAĞLAYICILI KOMPOZİTLER

ŞİMŞEK, Yunus Emre
Yüksek Lisans Tezi, İnşaat Mühendisliği Bölümü
Tez Yöneticisi: Doç. Dr. Mustafa ŞAHMARAN
Nisan 2013, 72 sayfa

Beton altyapılarının performansındaki düşüşler genellikle servis ömrü boyunca çeşitli bozulma mekanizmaları sebebiyle ortaya çıkabilecek çatlak oluşumlarıyla ilişkilendirilmektedir. Çoğu zaman, performans düşüklüğüne sebep olan yıpranmış bölümlerin hızlı bir şekilde onarılması gerekli olmaktadır. Bu sebeple, kısa sürede yeterli oranda dayanım kazanabilen, çevresel ve mekanik yüklemeler sonucu oluşan deformasyonlara karşı dayanıklı ve erken yaş rötre çatlaklarını engelleyebilen boyutsal kararlılığa sahip, sünek tamir malzemelerinin geliştirilmesi oldukça önem arz etmektedir. Bu çalışmada, bahsedilen tarzda bir malzemenin (erken dayanımı yüksek, tasarlanmış çimento esaslı kompozit – HES-ECC) performansı mekanik ve boyutsal kararlılık özellikleri incelenerek araştırılmıştır. Bunun için, farklı su - bağlayıcı malzeme ve cüruf - Portland çimentosu oranlarına sahip kompozit malzemeler üretilmiştir. Kompozit özelliklerinin süneklik ve erken yaş rötresi bakımından iyileştirilebilmesi için suya doygun hafif agregalar (LWA) karışımlarda kullanılan kum ile değiştirilmiştir. Deney sonuçları, bu çalışmada geliştirilen HES-ECC karışımlarının büyük çoğunluğunun altı saat sonunda 20 MPa'dan fazla basınç dayanımı ve minimum 6 MPa eğilme dayanımına ulaştığını göstermektedir. Ayrıca, HES-ECC karışımları önemli ölçüde düşüş gösteren otojen rötre şekil değiştirme kapasiteleriyle beraber, normal dayanıma sahip ECC numunelerine yakın seviyelerde şekil değiştirme sertleşmesi göstermiştir. Elde edilen bu özellikler erken yaş çatlaklarının oluşumunda tehlike arz etmemektedir. Tüm bu çelişkili parametrelerin biraraya getirilmesi HES-ECC'nin hızlı ve sağlam bir onarım için gerekli şartları sağladığını göstermektedir.

***Anahtar Kelimeler:*** Erken Dayanımı Yüksek Tasarlanmış Çimento Esaslı Kompozitler (HESECC); Hafif Agregalar (LWA); Mekanik Özellikler; Boyutsal Stabilite.

# TABLE OF CONTENTS

# LIST OF FIGURES

**Page**

# LIST OF TABLES

# LIST OF SYMBOLS/ABBREVIATIONS

CA                Continuous air

CW              Continuous water

ECC             Engineered cementitious composites

$e^{f\phi}$             Accounts for the changes in bridging force for fibers crossing at an inclined angle to the crack plane

ESEM          Environmental scanning electron microscope

f                 Snubbing coefficient

$f\left(\dfrac{a}{W}\right)$        Geometric calibration factor

FA               Fly ash

FRC             Fiber reinforced concrete

HPC             High performance concrete

HPFRCC       High performance fiber reinforced cementitious composites

HRWR         High range water reducing admixture

HVFA          High volume fly ash

IC                Internal curing

ITZ             Interfacial transition zone

$J'_b$             Complimentary energy

$J_{tip}$            Fracture energy of the mortar matrix

| | |
|---|---|
| $K_m$ | Fracture toughness of the mortar matrix |
| $L_f$ | Fiber length |
| LVDT | Linear variable displacement transducer |
| LWA | Light-weight aggregate |
| MAS | Maximum aggregate size |
| MIP | Mercury intrusion porosimetry |
| $p(z)$ | Centroidal distance from the crack plane |
| $P(\delta)$ | Pullout load versus displacement relation of a single fiber aligned normal to the crack plane |
| $p(\phi)$ | Probability density functions of the fiber orientation angle |
| PC | Portland cement |
| PVA | Poly-vinyl-alcohol |
| $P_Q$ | Applied load |
| R/C | Reinforced concrete |
| R/ECC | Reinforced ECC |
| RCPT | Rapid chloride permeability test |
| RH | Relative humidity |
| SAP | Super absorbent polymer |
| SEM | Scanning electron microscopy |
| $V_f$ | Fiber volume fraction |
| W/C | Water to cement ratio |
| W/CM | Water to cementitious materials ratio |

z                        Centroidal distance of a fiber from the crack plane

$\delta_0$                      Crack opening

$\phi$                      Orientation angle of the fiber

$\sigma_0$                      Maximum crack bridging stress

$\sigma_{fc}$                      First cracking strength of mortar matrix

$\delta_0$                      Crack opening

$\phi$                      Orientation angle of the fiber

# CHAPTER 1

# INTRODUCTION

## 1.1 General

Concrete material often cracks, and cracking significantly damages the durability properties of concrete. Thus, it is an issue of major concern in the construction industry. Deterioration mechanisms leading to cracking in concrete may involve environmental (e.g. freeze/thaw cycles, corrosion and different shrinkage types), external (e.g. poor workmanship and construction practices) and mechanical effects (e.g. fatigue) (Frangopol and Furuta, 2000; Narayan, 2007; Mays, 1992). Concrete may also lose its load carrying capacity or even spall and fail with the influence of more catastrophic impacts such as earthquakes, hurricanes and fire. This reduction in performance often requires rapid and effective repair of deteriorated sections.

Increasing repair, retrofit and maintenance costs of existing concrete structures is a growing concern. In the U.S. alone, the estimated cost for maintenance of deteriorated roads and bridges over the next 20 years is a staggering $1.8 trillion (AASHTO, 2002). In Asia, it is $2 trillion. In most European countries, the cost of repair already exceeds that of new construction (Li, 2005). Therefore, the design of cost-efficient, durable and high performance repair materials is extremely desirable for the sustainability of different infrastructure types such as bridge decks, highway pavements, parking structures, and airport runways.

When traffic congestion is factored into repairs, an ideal repair material needs to show high strength gain at early ages. The required time for a repair job is approximately six to eight hours, and construction is mostly done at night so that the road can be opened the next morning without any interruption in traffic flow. While high early compressive strength is an indispensable material property for repair materials, it also causes an increase in the elastic modulus and brittleness of the

material, which can facilitate the formation of cracks. Unfortunately, repairs made with conventional materials are more prone to cracking; almost half of traditional concrete repairs fail (Mather and Warner, 2004). In addition to the premature cracking of high early strength repair materials that might arise under several service conditions cracks also originate due to autogenous shrinkage (Whiting and Nagi, 1994). Differences in thermal gradients stand as one of the problematic issues for the design of truly resilient repair materials. Therefore, to be used as a repair material, concrete must gain compressive strength at early ages, show adequate flexural characteristics and compensate for the drawbacks (e.g. crack formation) caused due to the effects of different shrinkage mechanisms.

Engineered Cementitious Composites (ECC) are a special type of high performance fiber-reinforced cementitious composites featuring high ductility and damage tolerance under mechanical loading, including tensile and shear loadings (Li, 1997; Li, 2003). By employing micromechanics-based material optimization, tensile strain capacity in excess of 3% under uniaxial tensile loading can be attained with only 2% fiber content by volume (Li, 1997; Lin et al., 1999). Strain-hardening behavior, which is one of the material characteristics of ECC, is associated with the multiple tight cracking phenomenon of the brittle matrix. The formation of multiple microcracks with widths of less than 100 μm is an intrinsic material property of ECC. This phenomenon is self-controlled and not dependent on the reinforcement ratio. Multiple microcracking is realized through an increment in ductility that is considered one of the most influencing parameters for the durability of repair materials (Wang and Li, 2006). However, high early strength causes reductions in ductility due to increased paste maturity and its damaging effects on fiber and the fiber-matrix interface. In addition, increased early compressive strength may result in cracks caused due to several shrinkage types. Over the years, many researchers have concentrated on high early strength and fast-stiffening concrete materials and gathered invaluable information about how these properties were obtained (Seehra et al., 1993; Knofel and Wang, 1994). However, only a few studies target the simultaneous attainment of compressive strength and tensile ductility at early ages (Wang and Li, 2006; Li and Li, 2011). In these studies, high tensile ductility through saturated multiple microcracking was effectively achieved with the introduction of artificial flaws into the matrix. Thus, a similar approach was used throughout this

study in order to integrate tensile ductility and high early strength. Also to achieve this in the current study, pre-soaked LWAs were added into the mixtures; not only as artificial flaws to tailor the ductility of the matrix, but also as internal moisture reservoirs to minimize early age cracking due to increased paste maturity.

As briefly mentioned before, ideal repair material must meet certain compressive strength value especially at early ages. Despite its significance in repair materials, no certain specification in the existing standards was stated for minimum compressive strength requirement. Yet, several authorities suggested different minimum limits for compressive strength values depending on the specific construction need (Parker and Shoemaker, 1991; Kurtz et al., 1997; Federal Highway Administration (FHWA), 1999).

Concurrent attainment of high early strength, tensile ductility and low early age shrinkage is a challenging aim for repair materials due to conflicting design approaches of different properties. In the light of this aim, the thesis presents the performance analysis of a new repair material, High Early Strength Engineered Cementitious Composites (HES-ECC), which combine high early strength, tensile deformability and very low early age shrinkage characteristics. To date, there has been limited information available in the literature related to the performance of such materials. This study also aims to fill that knowledge gap.

## 1.2 Research Objectives and Scope

In this study, emphasis was placed on the design of high early strength ECC (HES-ECC), which can show characteristics superior to other repair materials currently available in the market. To do this, three mixtures with different ground granulated blast furnace slag (S) to Portland cement (PC) ratio (S/PC) and water to cementitious material ratio (W/CM) were produced. During the production of mixtures, pre-soaked expanded perlite was used as saturated lightweight aggregate (LWA). Maximum aggregate sizes (MAS) of LWA used in the mixtures were 2 mm and 4 mm. LWA replacement rates were 25% and 50% by volume. The current study is unique in that pre-soaked LWAs were utilized not only as artificial flaws to tailor the ductility of the matrix, but also as internal moisture reservoirs to minimize early age

cracking due to increased paste maturity. The testing program was composed of two phases. In the first phase, mechanical properties of the specimens were evaluated, and in the second, dimensional stability was investigated. Mechanical properties including compressive strength, flexural strength, flexural deformation and fracture toughness results were presented. The dimensional stability phase covered results obtained from autogenous shrinkage and drying shrinkage tests.

In Chapter 2, durability properties of HES concrete, application of ECC, and pozzolanic materials such as ground granulated blast furnace slag are discussed. In Chapter 3, experimental program, materials properties and tests performed on mechanical properties and dimensional stability of ECC are discussed. The results of the experimental studies are presented and discussed in Chapter 4. The conclusions of the research are represented in Chapter 5.

## CHAPTER II

## LITERATURE REVIEW AND BACKGROUND

### 2.1 Introduction

Nowadays, fast going constructions have created a need for early age improvement of concrete's strength. These types of constructions including localized repairs, replacement of busy intersections and major slip-form paving can show significant economical benefits because of completing the construction in shorter times. Also for structural components, removal of forms earlier than required or the post-tensioning application , and the process of curing in cold weather, have safety results as well as in cost savings economically. Also, as air travel worldwide continues to grow in Turkey and all over the world, there is an ever-increasing demand placed on airport infrastructure systems. Concrete pavements, for example, carry both larger volumes of aircraft traffic as well as higher loads than originally intended. This has resulted in the need for many pavements to be repaired or replaced. Repairing and returning these pavements to service quickly with only minimal disruption of their use are an economic imperative. As a result, High Early Strength Concrete (HES Concrete) has emerged to address these needs.

### 2.2 What is High Early Strength Concrete (HES Concrete)

HES concrete, also known as fast track concrete, gets the required strength at earlier time different than normal concrete. High early strength can be achieved by using ingredients and producing techniques of traditional concrete, but sometimes special materials or practices are required. The age at which concrete must develop its high strength is an important factor in the design of a mix. If high early strength is required, it can often be achieved by modifying an existing mix design to incorporate:

1. High early strength cement (CEM-I 52.5 R, Type –III cement or etc.)

2. High-cement content (400 to 600 kg/m$^3$)

3. Low ratio of water cementing materials (0.20 to 0.45 by mass)

4. High temperature for freshly mixed concrete

5. Higher temperature for curing

6. Suitable Chemical admixtures

7. Silica fume (or other supplementary cementing materials like slag, fly ash, etc.)

8. Curing with steam or autoclaving

9. Insulation for retaining the hydration heat

10. Special cements that hardens rapidly. (i.e. CEM I 52.5 R or TYPE-III cement)

The requirements of high early strength in terms of compressive strength and/or flexural strength of various DOTs in the US were reviewed. Presently, there is not any validated standard that explains the requirements for high early strength. The California Department of Transportation (Caltrans) determines that 2.76 MPa flexural strength is the minimum required strength to open a highway to service for full depth highway pavement repairs (Concrete Construction, 2001). The 2.76 MPa requirement is based on pavement design and the experience that the durability and life expectancy of the repaired pavement may be jeopardized if the slab is subjected to traffic prior to obtaining this strength. The New Jersey State Department of Transportation specified a minimum compressive strength of 20.7 MPa in 6 hours, and a minimum flexural strength of 2.41 MPa in 6 hours, for the "Fast-track mix" developed in mid of 1990's (Kurtz et al., 1997). The Michigan Department of Transportation (MDOT) specifies minimum compressive strengths of 13.8 MPa in 2 hours, 17.2 MPa in 4 hours, and 31.0 MPa in 28 days for prepackaged hydraulic fast-set materials used in structural concrete repairs. Moreover, MDOT indicates the physical requirements for prepackaged hydraulic fast-set materials for use in

structural concrete repairs, and the procedure to be followed by producers in order to have their products included on MDOT's Qualified Products List (MDOT QA/QC, 2003).

The compressive strength requirements at different ages by various DOT's and The Federal Highway Administration (FHWA) in USA are summarized in Figure 2.1.
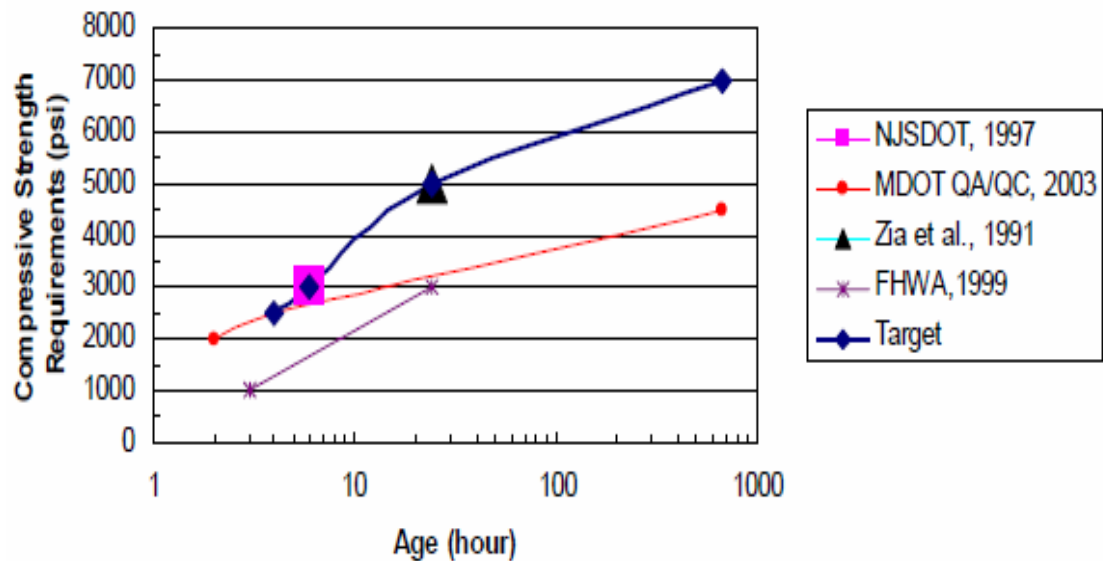


Figure 2.1 Compressive strength requirements at different ages (Li et al., 2006)

Furthermore, Parker and Shoemaker (1991) recommended a minimum 14 MPa compressive strength for road patching repair, that was assumed to be capable to prevent abrasion, cracking, deformation due to travelling when initially opened to traffic. A national research program report (Zia et al., 1991) which focuses on high performance concretes indicates three categories related with strength: (a) very early strength, (b) high early strength, and (c) very high strength. The very early strength concretes have minimum strength of 20.7 MPa in 4 hours after placing the concrete. And the high early strength concretes have a minimum compressive strength of 34 MPa in 24 hours after placement. Moreover, FHWA Manual of Practice: Materials and Procedures for Rapid Repair of Partial-Depth Spalls in Concrete Pavements (FHWA, 1999) suggests for Rapid setting Cementitious Concrete which has a minimum compressive strength of 7 MPa at 3 hours, 20 MPa at 24 hours, and initial set time of 15 minutes.

**2.3 Current Methods to Obtain High Early Strength**

As mentioned earlier, high early strength is normally achieved by using one or a combination of the factors mentioned in the section 2.2. Some general informations are explained below about HES-ECC in the point of view on cements and admixtures because they play the key roles in the functionality for obtaining high early strength quality. Detailed information about exact ingredients used in this study was given in Chapter 3.

**2.3.1 Cement**

To obtain high early strength, it is highly required to use a rapid hardening cement with high early strength. A Portland cement containing a high content of $C_3S$ and $C_3A$ to give rapid hardening and setting properties. High Early Strength Portland Cement only requires 3 days to show the strength that Ordinary Portland Cement shows in 7 days. High Early Strength Cement complies with the low alkali requirement specified by ASTM C150 and TS EN 197-1. High early strength cement is produced from Portland cement clinker and gypsum and may contain up to 5% mineral additions.

Hydraulic binders as; CEM I 52,5R, Type III and Type HE Portland cements are the most known cements used in constructions where a more rapid rate of strength gain is desirable. The strength gain of normal Portland cement is mainly contributed by the hydration of Tricalcium Silicate ($C_3S$) and Dicalcium Silicate ($C_2S$), which produces a Calcium Silicate Hydrate (C-S-H), also higher Tricalcium Aluminate ($C_3A$) content supports rapid hardening. By grinding the cement more finely, the resultant increased surface area that will be in contact with water means faster hydration and more rapid development of strength. By this means, Type III cement can develop strength much faster than Type I cement within the first 3-8 hours. The amount of strength gain of Type III cement over the first 24 hours is about double that of Type I cement (Neville and Brooks, 1987). SEM images of the hydrated Type III cement paste at 28 and 7 days can be seen in the Figure 2.2.
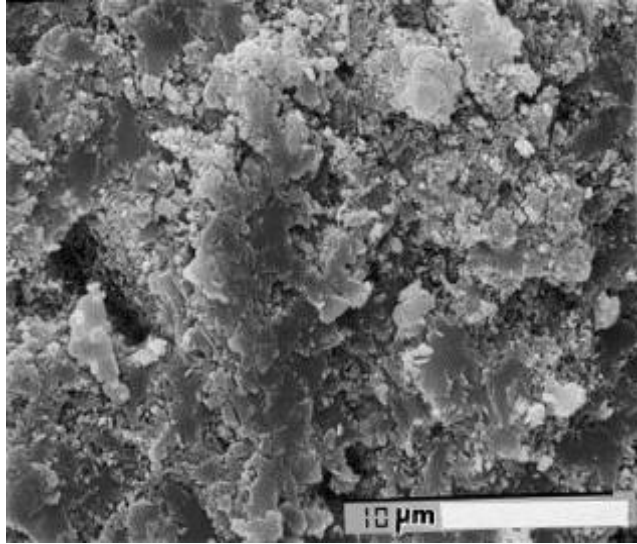
(a)
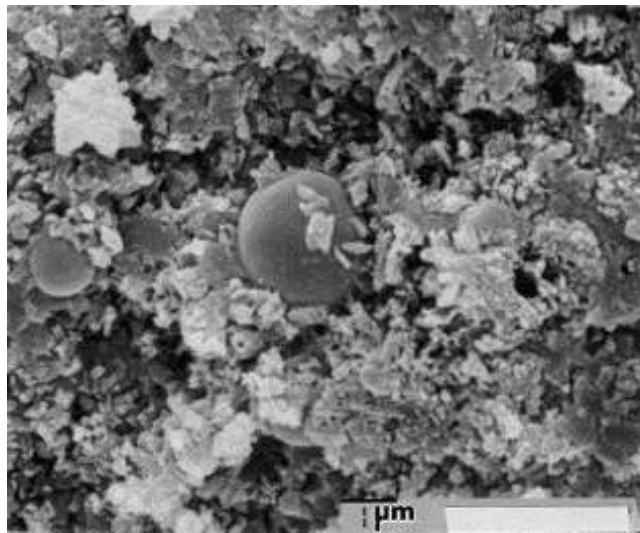


(b)

Figure 2.2 SEM image of the hydrated Type III cement paste at (a) 28 days (b) 7 days (Sarkar and Wheeler, 2001)

Also, Type HE cement provides high strength. It is chemically and physically similar to General Use Hydraulic Cement, except that its particles are more finely grounded. It is used when forms need to be removed promptly or when the structure must be put into service quickly. In cold weather, its use reduces the length of the curing period.

In this study, CEM I 52.5R which is a Portland cement type complying with TS EN 197-1 is used as hydraulic binder material. It consists of Portland cement clinker and a sulfate compound, which is needed as a setting regulator. The optimized production

process ensures a high degree of uniformity of the cement. As a low-chromium cement, a small amount of a chromium reducing additive may also be included. Properties CEM I 52.5 R is a fine, very bright special cement. Due to its high Portland cement clinker content, CEM I 52.5 R has a very high initial strength and high final strengths. The cement exhibits good compatibility and effectiveness with construction chemical additives such as plasticizers, retarders, accelerators,dispersion powders, etc., and is thus especially well suited for the production of dry mortar systems. The cement complies with EU Directive 2003/53/EC for low chromium levels.

Chemical admixtures also have an important key role while producing HES concrete mixtures on the points of strength and workability criterias. To improve the workability and increase the strength gain of mixture, lower water content is an important factor, to achieve this water reducing admixtures are required. Also, to increase strength at earlier ages accelerating admixtures play a key role. Moreover, admixtures for controlling the hydration heat allows time for concrete transportation from plant to the site, and provide adequate time for placement and finishing. The detail information on various chemical admixtures and their potential effects on material performance are reviewed in the section below:

### 2.3.2 Water-reducing Admixtures

A water-reducing admixture can effectively lower the water/cement ratio by reducing the water required to attain a given slump. Consequently, it improves the strength and impermeability of the cement matrix. The strength increase can be observed in as early as one day if excessive retardation does not occur (Ramachandran, 1996). Furthermore, since the cement is dispersed and a more uniform microstructure is developed, the compressive strength can be as much as 25% greater than that achieved by the decrease in w/c alone (Malhotra et al., 1989).

They also improve the properties of concrete containing marginal- or low-quality aggregates and help in placing concrete under difficult conditions (ACI Comm. 212, 1963). Water reducers have been used primarily in bridge decks, low-slump concrete overlays, and patching concrete.

Water-reducing admixtures can be categorized according to their active ingredients. There are the following:

1. Salts and modifications of hydroxylized carboxylic acids (HC type);

2. Salts and modifications of lignosulfonic acids (lignins); and

3. Polymeric materials (PS type). (ACI Comm. 212, 1991).

The basic role of water reducers is to deflocculate the cement particles agglomerated together and release the water tied up in these agglomerations, producing more fluid paste at lower water contents.

Water-reducing admixtures are often observed to increase the rate of shrinkage and creep of concrete, depending on the cement type and the particular admixture. However, after 90 days of drying, there is little difference in shrinkage compared to a control concrete (Nmai et al., 1998; Ramachandran et al., 1987). The shrinkage properties of the developed HES-ECC and related durability issues will be investigated in the subsequent research tasks.

### 2.3.3 Accelerating Admixtures

Accelerating admixtures accelerate the normal strength development and processes of setting and strength development. Regular accelerators are used to speed construction by permitting earlier attainment of sufficient strength to allow removal of formwork and to carry construction loads. Quick-setting admixtures provide setting times of only a few minutes. They are generally used in shotcreting applications and for emergency repair in general where very rapid development of rigidity is required. Accelerators are also beneficial during winter concreting because it can partially overcome the slower rate of hydration due to low temperatures and shorten the period for which protection against freezing is required (Edmeades and Hewlett, 1998, Mindess et al., 2002).

Accelerating admixtures can be divided into three groups:

(1) soluble inorganic salts

(2) soluble organic compounds, and

(3) miscellaneous solid materials (ACI Committee 212, 1991).

Many soluble inorganic salts can accelerate the setting and hardening of concrete to some degree, calcium salts generally being the most effective. Soluble carbonates, aluminates, fluorides, and ferric salts have quick-setting propertiesand they are commonly used in shotcreting applications. Calcium chloride is the most widely used because it is the most cost effective, while giving more acceleration at a particular rate of addition than other accelerators (Ramachandran, 1996). However, the use of calcium chloride will increase the rate of corrosion of metals embedded in concrete. The ACI Building Code places limits on the chloride content of concrete that preclude its use for both prestressed and reinforced concrete. Chloride-free accelerators should be used in such cases.

Organic compounds for most commercial uses include triethanolamine, calcium formate, and calcium (Rear and Chin, 1990). These compounds accelerate the hydration of tricalcium aluminate and produce more ettringite at early age. The reaction of triethanolamine with Portland cement is complex. Although listed as an accelerator, it can cause retardation or flash setting, depending on the amount used (Hewlett and Young, 1989).

Solid materials are not often used for acceleration. Calcium fluoroaluminate or calcium sulfoaluminate can be used as admixtures to obtain rapid-hardening characteristics. Additions of calcium aluminate cements cause Portland cements to set rapidly, and concrete can be "seeded" by adding fully hydrated cement that has been finely ground during mixing to cause more rapid hydration. Finely divided carbonates (calcium or magnesium), silicate minerals, and silicas are reported to decrease setting times (Ramachandran, 1996; Rixom and Mailvaganam , 1986; Rear and Chin, 1990; Mindess et al., 2002).

Although accelerating admixtures can be expected to increase early strength, the increase diminishes with time, and later strengths (at 28 days or more) are likely to be lower than the strength of concretes without an accelerating admixture (Ramachandran, 1996). This reduction in later strength is more pronounced when the initial accelerating effects are large.

Accelerating admixtures may also increase the rate of drying shrinkage and creep, although the ultimate values are not affected (Rixom and Mailvaganam, 1986). The early shrinkage leads to high tensile stresses in restrained repair material, resulting in cracking or interface delamination.

## 2.4 Applications of High Early Strength Concrete

High early strength concrete is sometimes used for prestressed-concrete to allow for early stressing; precast-concrete for rapid production of elements; cast in place construction ongoing with high speed; rapidly reusage of form; construction in cold weather; to reduce traffic downtime rapidly repairing of pavements; road paving with high early strength (fast track paving); bridge and tall building consructions and some other usage areas. In the Figure 2.3, there is a site application of High Early Strength Concrete for airport aprons and taxiway replacement at Philadelphia International Airport, Pennsylvania, USA and in Figure 2.4 shows a HES repairing concrete application on road pavements of I-75 Highway, Virginia, USA and lastly in Figure 2.5, there are HES-ECC applications for a bridge construction and a tall building In fast track pavement applications, use of high early strength mixtures allows traffic to be opened within a few hours after concrete placement.



Figure 2.3 Application of high early strength concrete for airport aprons and taxiway replacement at Philadelphia International Airport, Pennsylvania

(a)



(b)

Figure 2.4 HES repairing concrete application on road pavements (a) (Road patching at previous night), (b) opened to service on next day, I-75 highway, Virginia – USA

Generaly, repair material strength gain rate at the early age determines when the repaired structure can be opened to service. Different repair applications may have different strength requirements at different ages. For example, large deck patches are typically given a 24-hour curing; small deck patches generally use fast setting mortar

to open traffic after a number of hours; and for prestressed concrete beam ends repairs,



<div align="center">(a)                                    (b)</div>

Figure 2 .5 HES concrete were used in structures (a) San Mateo Bridge ,CA – USA and (b) Scotia Plaza, Toronto - CANADA.

both the early age strength and the 28 days strength are normally specified. To be suitable for various repair applications, the HES-ECC developed must meet the minimum strength requirements at both the early and late ages (Li, 2006).

When designing the mixtures with early strength capability, development of strength is not the single criteria that should be examined; and other characteristics should also be determined like durability, early-stiffening, autogenous shrinkage, drying shrinkage, rise in temperature, for compatibility with the project. Special curing procedures, such as fogging, may be needed to control cracking due to plastic-shrinkage (Pyle, 2001).

## 2.5 Engineered Cementitious Composites (ECC)

In recent years, in many of developed countries the general expenditure for

infrastructure repair and retrofit is reaching and is awaited to become to go beyond new construction expenditure in the near future. Most of Civil Engineers in industrialized countries (including Turkey) recently recorded that the general situation of roads, highways, bridges, infrastrucral systems and other publical works have continued to deteriorate and so growing usage by a expanding population and materials ageing. As counterbalance to this situation, there is an exact and urgent need for growing amounts of infrastructure repairing, and this kind of repairings must be durable.

High performance fiber reinforced cementitious composites (HPFRCC) are a group of fiber reinforced cement based composites that shows a special ability of flexibility and self-strengthen before failing. This special type of concretes were improved for the aim of solving the structural problems inherent with traditional concrete, on the aspect of its tendency for failure in a brittle situation under extreme loading conditions and its later time durability. As a result of their design and composition, HPFRCCs maintain the significant ability to strain hardened under extreme loading conditions.

For structural applications, HPFRCCs should exhibit at least a deflection hardening behavior (see Figure 2.6). High-performance FRCCs are most attractive for use in critical regions/elements that may be subjected to large inelastic deformations combined with moderate to high shear stress reversals. For instance, use of HPFRCCs
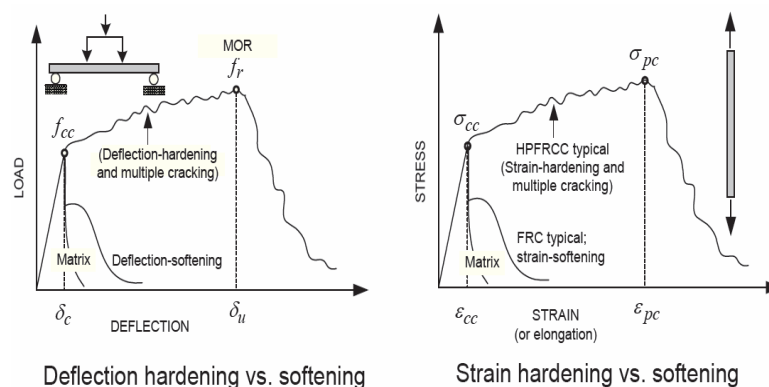


Figure 2.6 Hardening-softening behaviour of HPFRC under loading (Naaman and Reinhardt, 1996)

in critical regions of earthquake-resistant structures is a viable alternative to improve structural behavior while allowing significant reductions in steel reinforcement detailing. HPFRCCs have been shown to increase shear strength, displacement capacity, and damage tolerance in members subjected to large inelastic deformations combined with moderate to high shear stress reversals HPFRCCs show more resistance to cracking (see Figure 2.7) and operate considerably longer than normal concrete. (Naaman and Reinhardt, 1996)



a) Conventional RC shear wall            b) HPFRCC shear wall
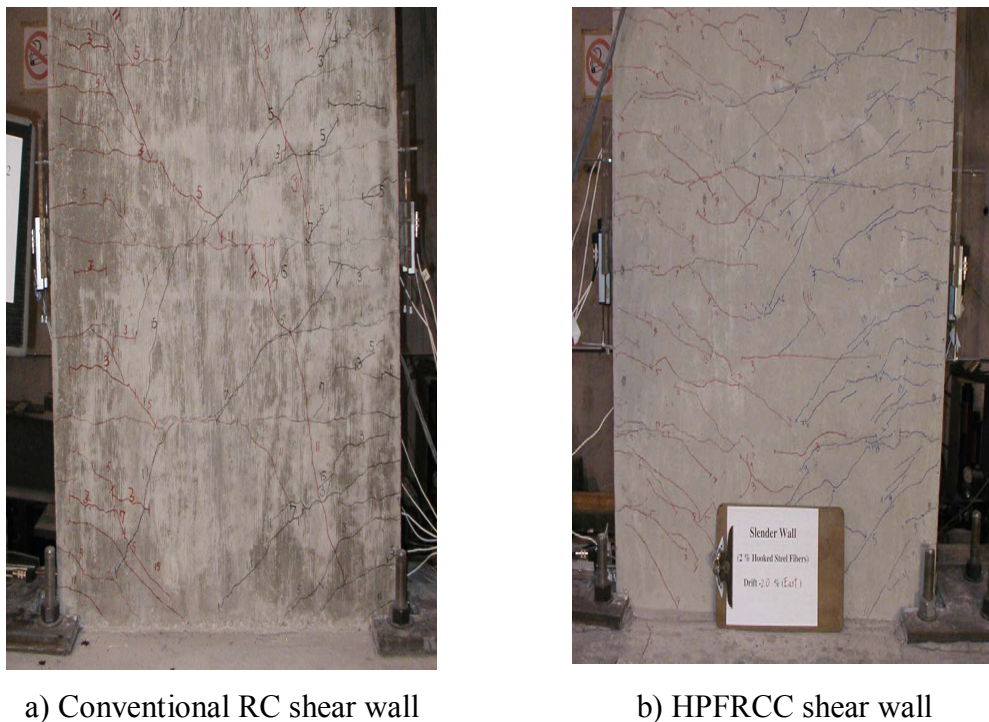
Figure 2.7 Crack distribution after failure (Parra, 2003)

At the end of the studies in the last two decades, a new type of material was developed known as Engineered-Cementitious-Composites (ECC), is a special type of high performance fiber reinforced cementitious composite which features high ductility and damage tolerance under mechanical loading conditions with tensile and shear loadings. The relative high cost remains an obstacle for wider commercial use of ECC. The replacement of Portland cement by fly ash and slag, and an increase in the amount and size of aggregate used in ECC production can lower its cost and enhance its greenness of composites, since the production of these materials needs less energy and causes less carbon dioxide emission than cement. By using the required designs, the required high tensile ductility, that is obtained by strain

hardening and multiple cracking, is induced to constraint sets on individual component properties. These components, which is, the fiber, the matrix, and the interface, are synergistically tailored to meet the requirements. (Li and Wang, 2006).

Typical mix proportion of ECC using a poly-vinyl-alcohol (PVA) fiber are given in below Table 2.1.

Table 2.1 Typical mix design of ECC material (Li and Wang, 2006).

| Cement | Water | Aggregate | Fly Ash | HRWR* | Fiber (%) |
|--------|-------|-----------|---------|-------|-----------|
| 1.00 | 0.58 | 0.80 | 1.20 | 0.013 | 2.00 |

*HRWR = High range water reducing admixture; all ingredients proportion by weight
except for fiber.

To acquire high performance, most of HPFRCCs stands on a high volume of PVA based fiber in contrast ECC needs less amounts, generally 2% by volume, of short, dis-continuous fiber. This less volume of fiber content, along with the common components, provides flexible operanational construction. Until the present time, ECC materials have been improved for self consolidation casting (Kong et al., 2003), extrusion (Stang and Li, 1999), shotcreting (Kim et al., 2003), and conventional mixing in a gravity mixer or conventional mixing truck (Lepech and Li, 2005).

Figure 2.8 below illustrates the behaviour for typical uniaxial tensile stress-strain curve of ECC which contains PVA fiber 2% by volume (Weimann and Li, 2003). The individual strain-hardening behavior after first cracking is accompanied by multiple microcracking. In Figure 2.9, also The crack width occurance during inelastic straining can be seen. Moreover, at ultimate load, the crack width remains smaller than 80 µm. This tight crack width is self controlled and, whether the composite is used in combination with conventional reinforcement or not, it is a material characteristic independent of rebar reinforcement ratio.
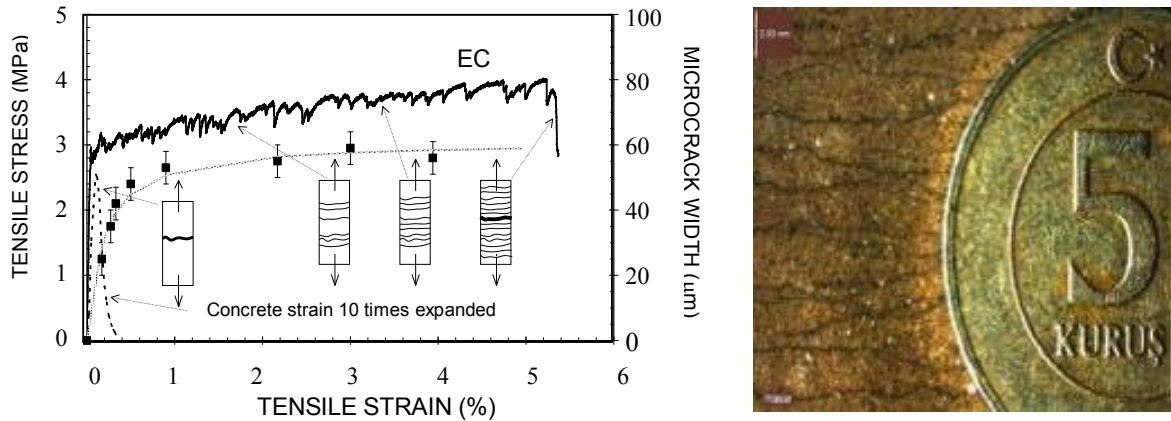
Figure 2.8 Crack width development of ECC and behaviour for typical uniaxial tensile stress-strain curve of ECC (Weimann and Li, 2003)

On the other hand, to control width of cracking, normal concrete and fiber-reinforced concrete stand on steel reinforcement. Under severe bending loads, an ECC beam deforms similar to a ductile metal plate through plastic deformation (see Figure 2.9). Under compressive loading, ECC materials show compressive strengths similar to high strength concrete (e.g. greater than 60 MPa) (Lepech and Li, 2005).



Figure 2.9 ECC's Behavioural Response against flexural loading

## 2.6 Design Criteria of Engineered Cementitious Composites (ECC)

The most important point while designing ECC material is to make sure strain hardening behaviour and the formation of multiple cracks under loading. So in this way, large deformations can easily be distributed over multiple micro-cracks. ECC material shows multiple micro-cracks that saturate the specimen while undergoing

strain-hardening during extreme tensile deformation. The formation of multiple steady state cracking is controlled by the bridging stress versus crack width opening relation along with the cracking toughness of the mortar matrix. To acquire this phenomenon the inequality shown in Equation-2.1 must be satisfied.

$$J_b^{'} = \sigma_0 \delta_0 - \int_0^{\delta_0} \sigma(\delta)d\delta \geq J_{tip} \approx \frac{K_m^2}{E_m} \qquad (2.1)$$

Where;

$J_b^{'}$ is the complimentary energy shown in Figure 2.10

$\sigma_0$ is the maximum crack bridging stress

$\delta_0$ is the corresponding crack opening

$J_{tip}$ is the fracture energy of the mortar matrix

$K_m$ is the fracture toughness of the mortar matrix

$E_m$ is the elastic modulus of the mortar matrix

In addition to the fracture energy criterion, a strength criterion expressed in Equation-2.2 must be satisfied. the tensile first cracking strength $\sigma_{fc}$ must not exceed the maximum bridging stress $\sigma_0$ (Li and Leung, 1992; Li and Wu, 1992),

$$\sigma_0 > \sigma_{fc} \qquad (2.2)$$

where;

$\sigma_0$ is the maximum crack bridging stress

$\sigma_{fc}$ is the first cracking strength of the mortar matrix.

Once an ECC mixture is chosen which sufficiently shows the two above criteria, the formation of multiple steady-state cracks, and strain-hardening performance, can be performed. However, in addition to forming these cracks, the material must also be designed to show crack widths which are not much more than the threshold limit point of 100 μm. This can be succeded through tailoring of the crack bridging versus

20

crack opening relation referenced in Equation-2.1. The maximum steady-state crack width showed during ECC multiple cracking can be accepted to be $\delta_0$ and the crack width corresponding to the maximum crack bridging stress, $\sigma_0$, as shown in Figure 2.10.
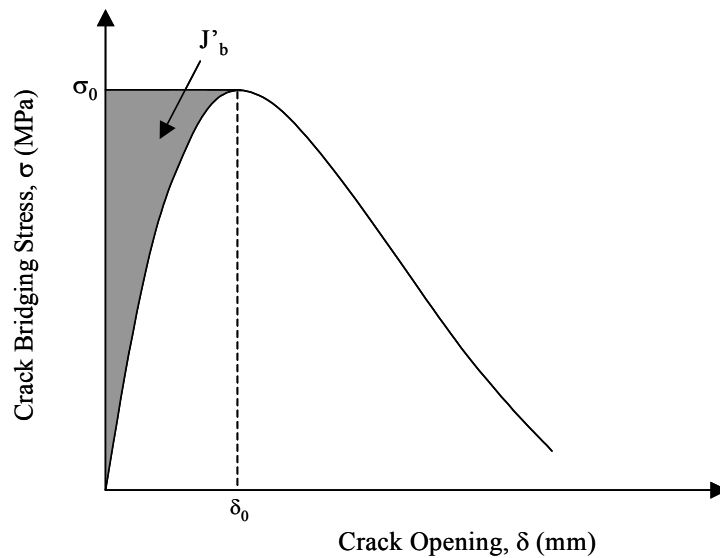
Figure 2.10  Crack bridging stress versus crack opening relation

## 2.7 Mechanical Properties and Durability of ECC

### 2.7.1 Fatigue

The performance of ECC has been investigated in high fatigue scenarios, such as rigid pavement overlay rehabilitation. In these overlay applications, reflective cracking through the new overlay is of greatest concern. Existing cracks and locally reduced load capacity in the substrate pavement can result in flexural fatigue within the overlay structure. To evaluate ECC performance as a rigid pavement overlay material, both ECC/concrete and concrete/concrete overlay specimens were tested in flexural fatigue (Zhang and Li, 2002). Similar advantages in the fatigue resistance of ECC have also been found in comparison to polymer cement mortars (Suthiwarapirak et al., 2002). Fatigue resistance of ECC for repair of viaducts subjected to train loading was studied by Inaguma et al. (2005). In fatigue-prone concrete infrastructure, the application of ECC materials may be able to significantly lengthen service-life, reduce maintenance events, and life cycle costs.

## 2.7.2 Spall Resistance

Greater resistance to spalling, brought about by reinforcing steel corrosion, can be achieved through the high ductility of ECC material. It is well known that once corrosion of steel reinforcing is initiated, corrosion debris expands against the surrounding concrete, creating a tensile circumferential stress state (i.e. hoop stress) in the cover concrete. This may lead to tensile radial cracking and subsequent spalling of the cover, resulting in a shortening of the structural service life. The spall resistance of ECC was investigated Kanda et al. (2003) and Miyazato and Hiraishi (2005) by pushing a tapered steel rod into a hole cast through an ECC slab in order to simulate the expansive force generated by a corroding rebar.

The test results showed that ECC accommodated the simulated expansion by "plastic yielding" through the formation of radial microcracks, while concrete fractured in a brittle nature under the expansive force. Figure 2.11 shows the signature damage and failure modes in ECC and concrete slabs after testing. Even with identical material compressive strengths, a significantly higher load (30 kN) was sustained by the ECC slab as compared to the concrete slab (~7 kN).



|              (a)                              /b)               |
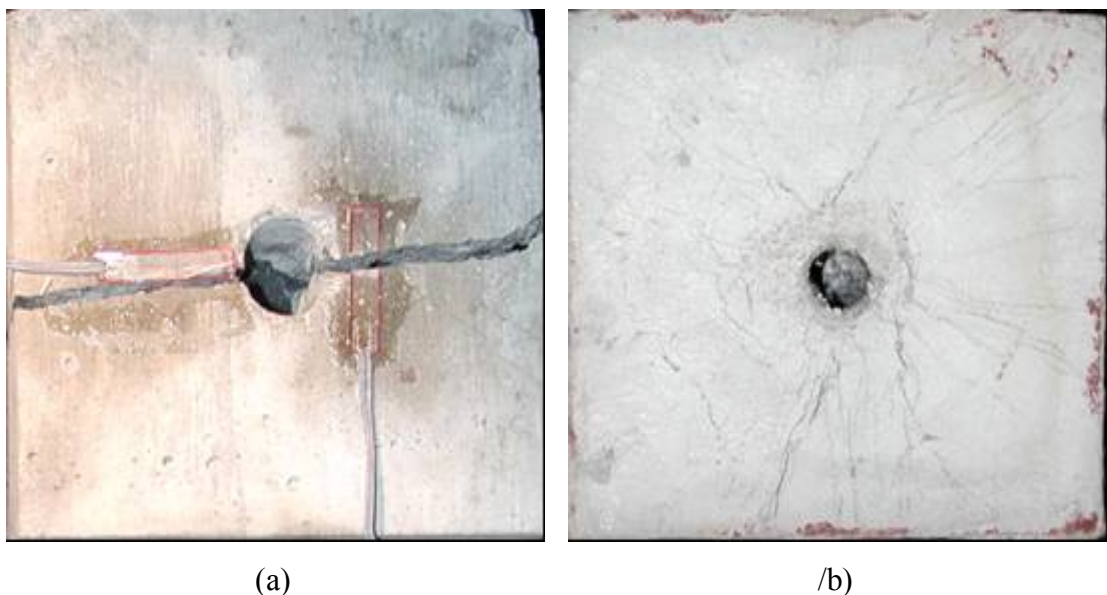
Figure 2.11 Failure modes of the slab (a) concrete, and (b) ECC (Kanda et al. ,2003)

## 2.7.3 Corrosion Resistance

Reinforcing steel bars embedded in concrete are usually well protected against corrosion by the high alkalinity of pore water because the steel surface is passivated in the presence of oxygen. Consequently, corrosion of reinforcement occurs which could lead to cover spalling and steel diameter reduction, and potentially diminishing of load capacity of the reinforced concrete member. This lack of load capacity of reinforcement and so as concrete inherently results in cracks which allow corroded particles to separate the cover, and results to failure for resisting the expansive force once corrosion starts.

With intrinsically tight crack width and high tensile ductility, ECC offers a significant potential to naturally resolving the corrosion related durability problem of reinforced concrete (R/C) structures. Concerned with the large number of microcracks within ECC in comparison to concrete, the rate of corrosion of reinforcing steel within an ECC matrix has been investigated and compared to R/C system (Miyazato and Hiraishi, 2005). Preloaded R/ECC and R/C beams were exposed to a chloride environment to accelerate the corrosion process. To determine the corrosion rate of ECC and concrete, macrocell and microcell corrosion rates were separately determined. The total (macro and micro cell) corrosion rate was measured to be less than 0.0004 mm/year but exceeded 0.008 mm/year in the steel reinforcement in the R/ECC and R/C beams respectively (see Figure 2.12).
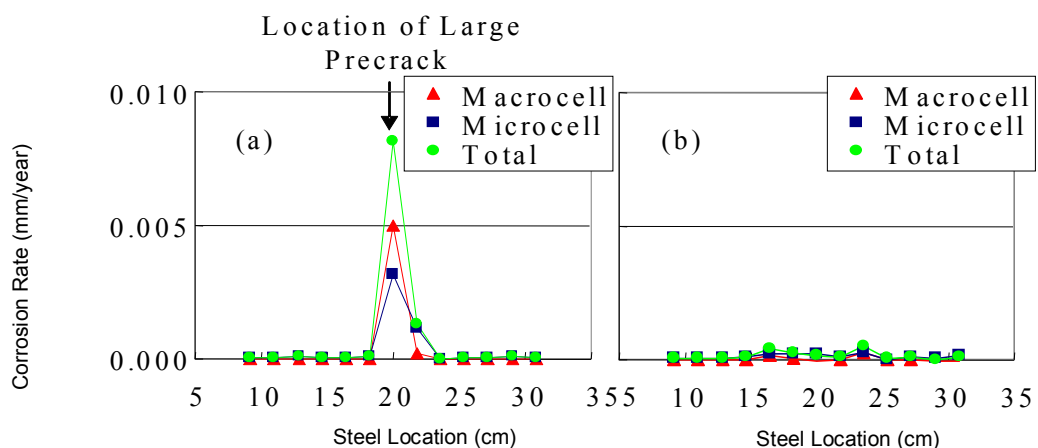


Figure 2.12 Microcell and macrocell corrosion rate measured for (a) R/C, and (b) R/ECC along the reinforcement bar length (Miyazato and Hiraishi, 2005)

### 2.7.4 Freeze Thaw and Salt Scaling Resistance

It is well known that the cyclical freeze-thaw cycles and the use of de-icing salts during winter are two of the major causes of rapid degradation in concrete pavements, bridge decks, parking structures, and similar structures. ECC used for this kind of structures must be resistant to cyclical freezing and thawing, and the effects of de-icing agents. It is known that a proper air-void system is generally needed in normal concrete to avoid internal cracking due to freeze-thaw cycles and scaling due to freezing in the presence of deicer salts.

Durability of non-air-entrained ECC specimens was tested by exposure to cycles of freezing thawing testing, in accordance with ASTM C666 (Li et al., 2003). Non-air-entrained concrete specimens were also tested as reference specimens. Non-air-entrained specimens were used as control since no air entrainment was added to the ECC mixtures.

After 110 cycles, the concrete specimens had severely deteriorated, requiring removal from the freeze-thaw machine, as mandated by the testing standard. However, all ECC specimens survived the test duration of 300 cycles with no degradation of dynamic modulus. Figure 2.13 shows the typical surface condition of the after 300 freeze-thaw cycles and fog room cured prismatic ECC specimens. This performance results in a durability factor of 10 for concrete compared to 100 for ECC, as computed according to ASTM C666 (1991).



(a) fog room curing            (b) after 300 freeze-thaw cycles
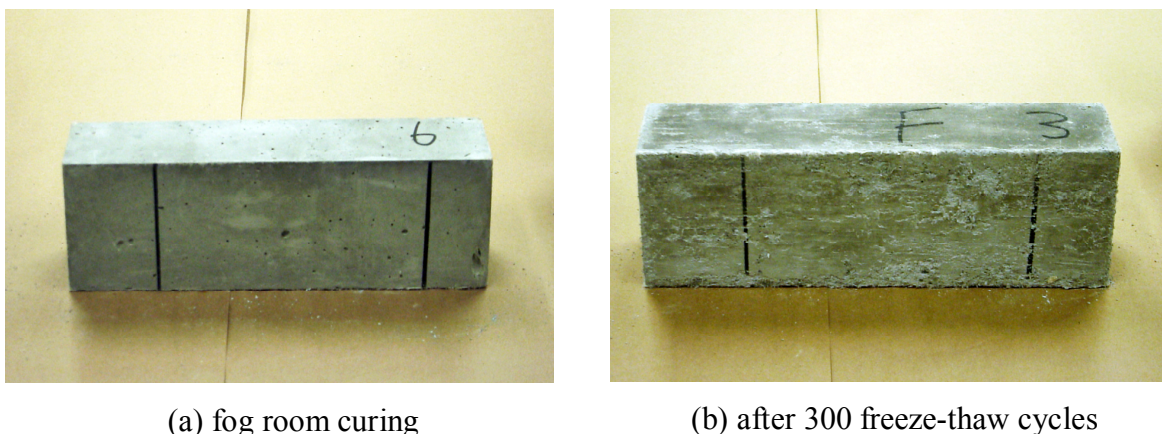
Figure 2.13 - ECC specimen surface appearance after (a) normal curing and (b) freeze-thaw cycles (Şahmaran and Li, 2007).

### 2.7.5 Durability under Extremely Harmfull Environments

In contrast to freeze thaw tests which are designed to simulate temperature changes in winter conditions, hot water immersion tests were conducted to simulate the long term effects of hot and humid environments. To examine the effects of environmental exposure, hot water immersion was performed on individual fibers, single fibers embedded in ECC matrix, and composite ECC material specimens (Li et al., 2004). Specimens for both individual fiber pull-out and composite ECC material were cured for 28 days at room temperature prior to immersion in hot water at 60 °C for up to 26 weeks.

After 26 weeks in hot water immersion, little change was seen in fiber properties such as fiber strength, fiber elastic modulus, and elongation. The tensile strain capacity of the ECC dropped from 4.5% at early age to 2.75% after 26 weeks of hot water immersion. While accelerated hot weather testing does result in lower strain capacity of ECC, the 2.75% strain capacity exhibited after 26 weeks remains over 250 times that of normal concrete.

Şahmaran and Li (2008b) investigated the durability of ECC under high alkaline environment. The performance of ECC under high alkaline medium was tested according to ASTM C1260-94 (1994). The length change of the ECC bars was measured up to 30 days. Figure 2.14 shows expansive behavior of the ECC.
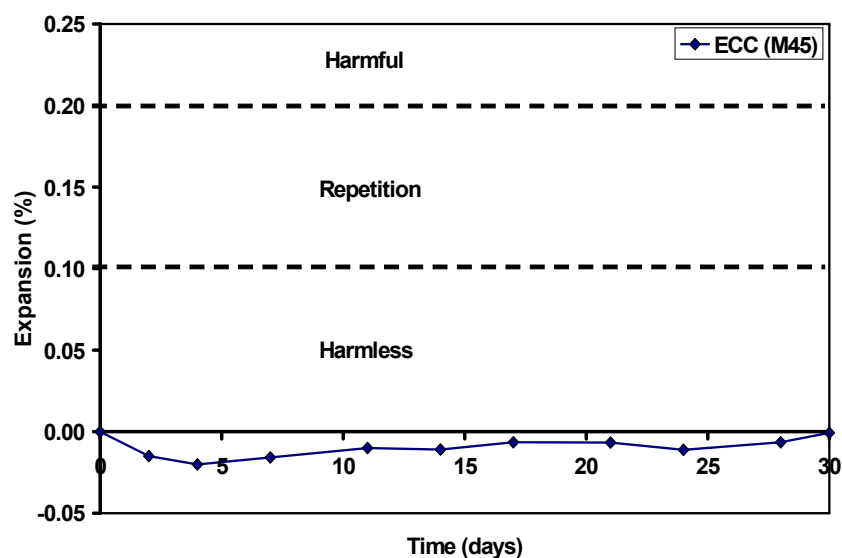


Figure 2.14 Expansion time histories for ECC (ASTM C1260-94)
(Şahmaran and Li, 2008)

## 2.8 Applications of ECC

In this section, to illustrate the versatility of ECC in real world applications, a number of recent/on-going projects involving the use of ECC are briefly highlighted. In 2007, a road pavement repair application (see Figure 2.15) was conducted by VDOT (Virginia Department of Transportation).



(a)



(b)

Figure 2.15  I-295 Repaving and Repairs , (a) Patching application, (b) Curing of patched lane, VDOT, USA 2007

The name of the project was "I-295 Repaving and Repairs" . In this application, VDOT planned the patched road to be opened to service in 6 hours. They used a type

of HES-ECC whose mixing proportion was defined by VDOT itself (I-295 Repaving and Repairs – Recently Completed Projects, VDOT, 2007).

During the application they applied compressive tests to the samples taken from the batching of repairing. And the data was tabulated as as shown in the Table 2.2.

Table 2.2 Compresive test results of samples from patched lane, VDOT, 2007

| Time from Batching | Time from Placing | Strength - MPa (cylinders on Slab) |
|---|---|---|
| 4 h 23 min | 3 h 23 min | 7,68 |
| 5 h 17 min | 4 h 17 min | 16,28 |
| 5 h 19 min | 4 h 19 min | 13,00 |
| 5 h 54 min | 4 h 54 min | 16,11 |
| 5 h 57 min | 4 h 57 min | 19,05 |
| 6 h 20 min | 5 h 20 min | 16,49 |
| 6 h 21 min | 5 h 21 min | 20,45 |
| 7 h 17 min | 6 h 17 min | 21,43 |
| 7 h 19 min | 6 h 19 min | 25,07 |

Figure 2.16 below shows the repair of the Mitaka Dam in Hiroshima-Prefecture, Japan in April, 2003 (Sakata et al., 2004). This dam is over 60 years old, with a severely damaged concrete surface.  Cracks, spalling, and water leakage were concerns that prompted the use of ECC as a water-tight cover layer.  This 20 mm layer was applied by spraying the ECC material directly onto approximately 600 m$^2$ of the upstream dam surface.

Also in Japan ECC has been used in structural applications as coupling beams (Maruta et al., 2005) within high rise concrete construction.  Due to the high energy absorption capacity of steel reinforced ECC material, the application of this material in coupling beams which connect adjacent core walls is very advantageous for high rise buildings in seismic regions.
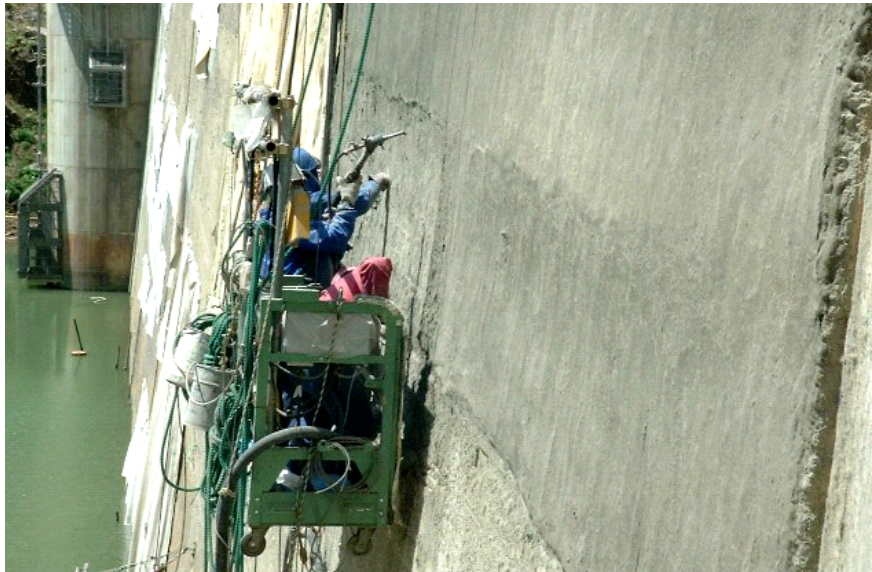
Figure 2.16 Spray repair of the Mitaka Dam, Japan with
ECC for water-proofing (Sakata et al., 2004)

The recent development of precast ECC coupling beam elements by Kajima
Corporation in Japan can be easily integrated into current seismic construction
practices. Currently two high-rise buildings in Tokyo, Japan have been built
integrating ECC coupling beams (Figure 2.17).



Figure 2.17 The Nabeaure Tower in Yokohoma, Japan uses precast ECC coupling
beams in building core for seismic resistance (Sakata et al., 2004)

Also the most recent field application of ECC in the US is with a bridge "link slab"
completed in cooperation with MDOT in 2005 (Figure 2.18). Within this "link slab",
the material ductility of ECC is leveraged to replace problematic expansion joints

within simply support multi-span bridges with a ductile ECC slab which links the adjacent simple spans (Li et al., 2005). In this project, about 32 m$^3$ of ECC were cast in place using standard ready-mix concrete trucks to build the first ECC link slab in US. With a strain capacity exceeding 2%, these composites can be used to replace traditional steel expansion devices and can fully accommodate the thermal deformations of adjacent bridge spans.



(a)



(b)

Figure 2.18  ECC link-slab on Grove Street Bridge, Michigan, USA, (a) during construction, (b) after construction, (Li et al., 2005).

# CHAPTER 3

# EXPERIMENTAL PROGRAM

## 3.1 Materials

## 3.1.1 Cement

The cement (C) used in all mixtures was a normal portland cement CEM I 52.5R, which correspond to TS EN 197-1 CEM I type cement. It has a Blaine fineness of 460 $m^2$/kg. Chemical composition and physical properties of cement are presented in Table 3.1.

Table 3.1 Chemical properties of Portland cement and slag

| Chemical Compositions | PC | S |
|---|---|---|
| CaO | 65.7 | 35.1 |
| $SiO_2$ | 21.6 | 37.6 |
| $Al_2O_3$ | 4.1 | 10.6 |
| $Fe_2O_3$ | 0.26 | 0.28 |
| MgO | 1.3 | 7.9 |
| $SO_3$ | 3.3 | 2.9 |
| $K_2O$ | 0.77 | 1.1 |
| $Na_2O$ | 0.19 | 0.24 |
| Loss on Ignition | 3.2 | 2.8 |
| $SiO_2+Al_2O_3+Fe_2O_3$ | 25.9 | 48.4 |
| **Compound compositions** | | |
| $C_3S$ | 65.2 | - |
| $C_2S$ | 16.7 | - |
| $C_3A$ | 10.3 | - |
| $C_4AF$ | 0.79 | - |
| **Physical Properties** | | |
| Specific Gravity | 3.06 | 2.8 |
| Blaine Fineness ($m^2$/kg) | 460 | 425 |

### 3.1.2 Mineral Admixtures

### 3.1.2.1 Ground Granulated Blast Furnace Slag

Ground Granulated Blast Furnace Slag (hereafter called by Slag - S) was supplied from Iskenderun Iron–Steel Factory in Turkey. Its chemical oxide composition is given in Table 3.1. The specific gravity of slag was 2.79 g/cm$^3$ The slag was ground granulated in Iskenderun Cement Factory to have a Blaine specific surface area about 425 m$^2$/kg. According to ASTM C 989 (2009) hydraulic activity index, the slag used was classified as a category 80 slag. Particle size distribution of slag obtained by using the laser diffraction is shown in the Figure 3.1. To identify morphological characteristics of slag, it was analyzed with SEM and the resulting photograph is presented in Figure 3.1.
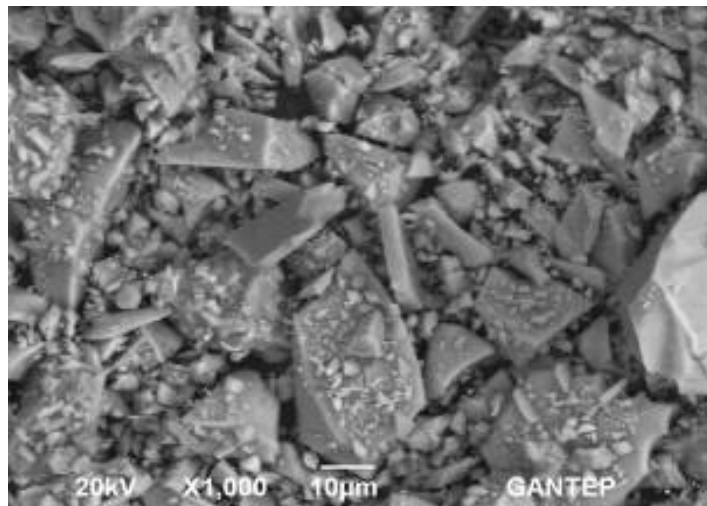


Figure 3.1 Particle morphology of slag determined by SEM

### 3.1.3 Aggregate

According to micromechanic-based design of ECC, exhibiting ductile and showing a large crack number, but small in width, of cementitious composites a low fracture toughness of the matrix is required. However, with the increasing of maximum grain size of aggregate, increase in toughness of the matrix is appeared and as a result, to obtain suitable ECC, aggregate grain size is limited (Li et al.,1995).

Therefore, so far, ECC has been produced successfully with an average grain size of about 110 μm (Li et al., 1995). Using high volumes of industrial by-product in the

production of ECC decreases matrix fracture toughness and provides freedom of changing aggregate size. It is very important to produce ECC from normal size local sources of aggregate in terms of widespread application for both literature and our country. For this purpose, in the production of ECC, fine quartz (see Figure 3.2) with a nominal aggregate size (MAS) of 400 μm was obtained from local sources in Turkey's resources. Water absorption capacity and specific weight of quartz aggregate used is 0.3% and 2.60, respectively.



Figure 3.2 A view of quatz sand aggregate

### 3.1.4 Expanded Perlite Lightweight Aggregate

The lightweight aggregate used in this study was expanded perlite type commercially manufactured. The expanded coarse perlite (C_LWA) which have MAS of 2 to 4 mm used in this study had water absorption capacity of nearly 144% and specific gravity of 0.88, these values were 131% and 0.92 in the case of fine perlite (F_LWA) which have MAS of 1 to 2 mm.

Perlite is a siliceous volcanic glass, the volume of which can expand substantially under the effect of heat. The perlite used consisted mainly of about 75% SiO2 and 13% $Al_2O_3$. When heated above 900 °C, its volume increases up to 35 times of the

original volume. As a result of this volume increase, absorption of the expanded perlite is significantly high. Moreover, the density of expanded perlite is very low (850 ± 25 kg/m3). As seen from Figure 3.3, the particle sizes (ranges from 0.1 to 5 mm) have a quasi-spherical shape.



Figure 3.3 A view of expanded coarse perlite (LWA)

### 3.1.5 Chemical Admixtures

To improve the workability of ECC mixtures, Glenium 51, high range water reducing admixture (HRWR – polycarboxylate ether as an active ingredient with 1.1 gr/cm$^3$ specific gravity and 40% solid content) produced by BASF Construction Chemicals was used.

It is consistent with the data tabulated Table 3.1.3.2 in TS EN 934-2: High range water reducing / Super plasticizer Concrete Admixture and Table 7 in ASTM C 494 Type F: High range water reducing / Super plasticizer Concrete Admixture Standards.

Here are some benefits and advatages of Glenium 51:
  ✓ Improves concrete's early and final compressive and flexural strengths

33

- ✓ Improves concrete's mechanic properties like carbonation, resistance to chlorine ion attack, resistance to aggressive chemicals, shrinkage, and creeping.

- ✓ Enables the production of low water/cement ratio, low segregation and leaching risk.

- ✓ Enables production of high early strength concrete even in low temperatures.

- ✓ Minimizes stripping time.

- ✓ Improves wear resistance of concrete by reducing segregation and bleeding.

- ✓ Reduces application periods of resin based pavement systems on new concrete with

- ✓ its low water/cement ratio, high early strength, and bleeding reduction properties.

- ✓ Increases Freezing - Thawing resistance of concrete.

- ✓ Reduces curing time and curing temperature in the production of precast elements.

- ✓ Can be used with all cement types.

- ✓ Shows less sensitivity to material differentiation.

Also, calcium nitrate salt based accelerator (Pozzolith 326 B) with the density of 1,316 - 1,376 kg/liter was used to fasten the reactions between water and cement especially when the initial set was reached.

It is consistent with the TS EN 934-2 Table 6: Set Accelerating Concrete Admixture and with ASTM C 494 Type C and E: Set Accelerating Concrete Admixture Standards.

Pozzolith 326 B goes into reaction with cement. When it is added to the mixture, it is absorbed by cement particles. Pozzolith 326 B accelerates the reaction between cement and water at the start of set and increases hydration temperature. As a result, setting of concrete is accelerated and its early strength is positively affected. It reduces concrete's initial and final set time compared to concrete without admixture. Especially in cold weathers, protects concrete from freezing effect by giving early strength.

### 3.1.6 Polyvinyl Alcohol (PVA) Fiber

Although various fiber types have been used in the production of ECC, PVA fiber was used in this study (see Figure 3.4). The use of PVA fiber was decided based on and PVA-ECC represents the most practical ECC used in the field (Li et al., 2001; Kunieda and Rokugo, 2006) at the present.



Figure 3.4 PVA fiber used in the production of ECC

PVA fibers have attracted most attention due to the outstanding composite performance and economics consideration. The dimensions of the PVA fiber are 8 mm in length and 39 μm in diameter. The nominal tensile strength and elastic modulus of the fiber is 1620 MPa and 42,8 GPa respectively and the density of the fiber is 1300 kg/m3. The mechanical and geometric properties of PVA fibers are summarized in Table 3.2. The PVA fiber is surface-coated by hydrophobic oil (1.2% by weight) in order to reduce the fiber/matrix interfacial bond strength. To account for material inhomogeneity, a fiber content of 2% by volume in excess of the calculated critical fiber content has been typically used in the mix design. These decisions were made through ECC micromechanics material design theory and had been experimentally demonstrated to produce good ECC properties in previous investigations (Li et al., 2002; Kong et al., 2003).

Table 3.2 Mechanical and geometric properties of PVA fibers

| Fiber Type | Nominal Strength (MPa) | Apparent Strength (MPa) | Diameter (μm) | Length (mm) | Elastic Modulus (GPa) | Ultimate Strain (%) | Specific Weight kg/m³ |
|---|---|---|---|---|---|---|---|
| PVA | 1620 | 1092 | 39 | 8 | 42.8 | 6.0 | 1300 |

## 3.2 Materials and Mixture Proportions

As mentioned in the introduction, an ideal repair material must meet certain compressive strength values, especially at early ages. However, despite its significance in repair materials, there is no specification for minimum compressive strength in the existing standards. Several authorities suggest different minimum limits for compressive strength values, depending on the specific construction need. According to Parker and Shoemaker, 13.8 MPa of initial compressive strength is adequate for a repair material to be resistant against several types of deformation (Parker and Shoemaker, 1991). The New Jersey State Department of Transportation (NJDOT) suggests 20.7 MPa of compressive strength at the age of six hours for a "fast-track mix" developed in the mid-1990s (Kurtz et al., 1997 and Kurtz et al., 2001). For rapid-setting cementitious concrete, 6.9 MPa and 20.7 MPa of compressive strength were recommended at three and 24 hours, respectively, by the Federal Highway Administration (Li, 2002). In the present study, the minimum requirement for compressive strength was agreed to be at least 20 MPa at the end of six hours.

In order to meet the specified compressive strength without sacrificing desired ECC material properties (i.e superior tensile ductility) several trial mixtures were designed with consideration for micromechanical design constraints. As a result of the preliminary studies, three different HES-ECC mixtures with two water to cementitious material ratios (W/CM) (i.e. 0.23 and 0.34) and slag to Portland cement ratios (S/PC) (i.e. 0.60 and 0.84) were selected. The mixture proportions for the three HES-ECC mixtures are presented in Table 3.3 below. The ingredients used in the mixtures were CEM I 52.5R high early strength Portland cement (PC), ground granulated blast furnace slag (S), silica sand, expanded lightweight perlite aggregate,

polyvinyl-alcohol fibers (PVA), water, high range water reducing admixture (HRWRA) and accelerating admixture (AA). The physical and chemical characteristics of PC and S are presented in Table 3.1.

Table 3.3 HES-ECC mixture proportions

| Ingredients, (kg/m³) | HES-ECC-1 | | | | | HES-ECC-2 | | | | | HES-ECC-3 | | | | |
|---|---|---|---|---|---|---|---|---|---|---|---|---|---|---|---|
| | Control | C_LWA | | F_LWA | | Control | C_LWA | | F_LWA | | Control | C_LWA | | F_LWA | |
| | | 25% | 50% | 25% | 50% | | 25% | 50% | 25% | 50% | | 25% | 50% | 25% | 50% |
| Total water | 298 | 298 | 298 | 298 | 298 | 299 | 299 | 299 | 299 | 299 | 300 | 300 | 300 | 300 | 300 |
| Portland Cement | 719 | 719 | 719 | 719 | 719 | 819 | 818 | 819 | 818 | 819 | 894 | 894 | 894 | 894 | 894 |
| Slag | 600 | 600 | 600 | 600 | 600 | 493 | 493 | 493 | 493 | 493 | - | - | - | - | - |
| Quartz sand | 587 | 439 | 293 | 439 | 293 | 598 | 449 | 300 | 449 | 300 | 976 | 732 | 488 | 732 | 488 |
| LWA (Perlite) | - | 50.0 | 100 | 50.0 | 100 | - | 51.0 | 102 | 51.0 | 102 | - | 84.0 | 168 | 84.0 | 168 |
| PVA fiber | 26.0 | 26.0 | 26.0 | 26.0 | 26.0 | 26.0 | 26.0 | 26.0 | 26.0 | 26.0 | 26.0 | 26.0 | 26.0 | 26.0 | 26.0 |
| HRWR | 13.8 | 10.8 | 8.6 | 10 | 8.2 | 12.6 | 10.1 | 8.7 | 9.7 | 7.9 | 9.2 | 7.1 | 5.1 | 5.3 | 3.9 |
| AA | 12.3 | 12.3 | 12.3 | 12.3 | 12.3 | 12.3 | 12.3 | 12.3 | 12.3 | 12.3 | 12.3 | 12.3 | 12.3 | 12.3 | 12.3 |
| Volumetric mass | 2256 | 2155 | 2057 | 2154 | 2057 | 2260 | 2158 | 2060 | 2158 | 2059 | 2218 | 2055 | 1893 | 2054 | 1892 |
| Total [W/(C+S)] | 0.23 | 0.23 | 0.23 | 0.23 | 0.23 | 0.23 | 0.23 | 0.23 | 0.23 | 0.23 | 0.34 | 0.34 | 0.34 | 0.34 | 0.34 |
| IC [W/(C+S)]* | - | 0.08 | 0.17 | 0.08 | 0.15 | - | 0.09 | 0.17 | 0.08 | 0.16 | - | 0.21 | 0.41 | 0.19 | 0.37 |
| Effective [W/(C+S)] | 0.23 | 0.31 | 0.40 | 0.31 | 0.38 | 0.23 | 0.32 | 0.40 | 0.31 | 0.39 | 0.34 | 0.55 | 0.75 | 0.53 | 0.71 |
| LWA/total sand | - | 0.25 | 0.50 | 0.25 | 0.50 | - | 0.25 | 0.50 | 0.25 | 0.50 | - | 0.25 | 0.50 | 0.25 | 0.50 |
| S/C | 0.84 | 0.84 | 0.84 | 0.84 | 0.84 | 0.60 | 0.60 | 0.60 | 0.60 | 0.60 | - | - | - | - | - |

*: Internal curing (IC) water to cementitious material (CM = Cement+Slag) ratio

In the mixtures, fine silica sand with a maximum aggregate size (MAS) of 400 µm was utilized, along with pre-soaked expanded fine and coarse perlite with MAS of 2.0 mm and 4.0 mm, respectively. Polycarboxylate ether type HRWRA with a specific gravity of 1.1 and 40% solid content was added to the mixtures until favorable fresh mortar characteristics were visually observed.

Calcium nitrate salt based accelerator with the specific gravity of 1.3 was used to fasten the reactions between the water and cement, especially when the initial set was reached. PVA fibers with a diameter of 39.0 µm and a length of 8.0 mm were purposely manufactured with a tensile strength (1620 MPa), elastic modulus (42.8 GPa), and maximum elongation (6.0%) matching those needed for strain-hardening performance.

The surface of the PVA fibers was coated with hydrophobic oiling agent (1.2% by weight) to reduce interfacial chemical bond strength between fiber and matrix with the aim of attaining strain hardening-performance (Li, 2002). The expanded coarse perlite (C) used in this study had water absorption capacity of nearly 144% and specific gravity of 0.88, and values for the fine perlite (F) were 131% and 0.92. The effects of saturated LWA usage on different shrinkage and mechanical properties were monitored on HES-ECC mixtures containing 25% (C or F_25%) and 50% (C or F_50%) of LWA replacements, by total aggregate volume (Figure 3.5). HES-ECC mixtures without LWAs (control) were also produced for comparison purposes.



Figure 3.5: View of LWA distribution throughout cross sections

## 3.3 Specimen Preparation and Testing

In this study, a Hobart type mixer (Figure 3.6) with 20-liter capacity was used in preparing all HES-ECC mixtures. Solid ingredients, including cement, mineral admixture (S) and aggregate, were first mixed at 100 rpm for a minute. Water, HRWR and AA admixtures were then added into the dry mixture and mixed at 150 rpm for one minute and then at 300 rpm for another two minutes to produce a consistent and uniform HES-ECC matrix (without PVA fiber). PVA fiber was added in last and mixed at 150 rpm for an additional three minutes.



Mixing of solid ingredients                    Water addition

HRWR addition                    Fiber addition

Figure 3.6 Production of ECC by using Hobart type mixer

To be used in flexural and compressive strength tests, prism and cubic specimens with the dimensions of 360×50×75 mm and 50 mm were produced from each HES-ECC mixture, respectively. The tests were performed by using four prism specimens for flexural and three cubic specimens for compressive strength tests at the ages of 6 hours, 24 hours, 7 days and 28 days.

The specimens that were intended to be tested were kept in laboratory medium at $50 \pm 5\%$ RH, $23\,^{\circ}$C.The rest of the specimens were stored in plastic bags at $95 \pm 5\%$ RH, $23 \pm 2\,^{\circ}$C (see Figure 3.7).



Figure 3.7 Moist curing of HES-ECC specimens after production

### 3.3.1 Compressive Strength

Twenty cubic samples (5x3 specimens for the each ages of 6 and 24 hourses and 7 and 28 days testing) of 50 mm were cast from each HES-ECC mixtures. The compression test was carried out on the cubic specimens by using a 3000 kN capacity testing machine in accordance with ASTM C39 (2003) (Figure 3.8). HES-ECC cubic samples were tested for compressive strength measurement at the age of 6 and 24 hourses and 7 and 28 days.

Figure 3.8 Compression testing machine and cubic samples

## 3.3.2 Flexural Performance

Flexural parameters were measured by using four-point bending tests performedon a closed-loop controlled material test systemwith a loading rate of 0.005 mm/s. The flexural loading was applied from span length of 304 mm and central span length of 101 mm. During the flexural tests, the load and mid-span deflection were recorded on a computerized data recording system (Figure 3.9).
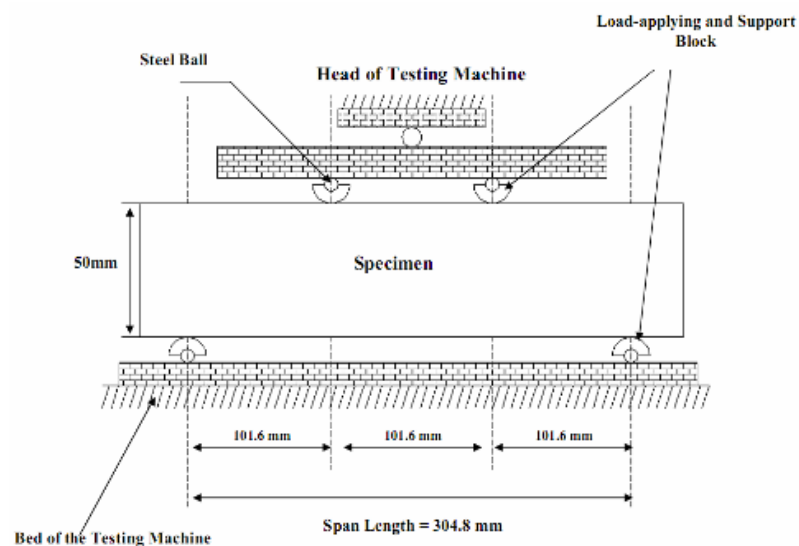


Figure 3.9 Four point bending test setup for flexural performance

The flexural deflection capacity of specimens was measured with the help of a LVDT placed on the test set-up. In the flexural stress–deformation curves, the maximum stress is defined as the flexural strength (modulus of rupture — MOR), and the corresponding deflection is defined as the flexural deformation capacity.

After bending tests, crack widths on the surface of the specimens were also measured by using a macroscope (Figure 3.10).



Figure 3.10 Controling for crack widths of specimens after tested by four-point test

### 3.3.3 Fracture Toughness

For toughness tests, prismatic mortar specimens (without PVA) with the same dimensions used in flexural strength test were utilized (Figure 3.11). In the standards, there is no specified measure of stress intensity factor of cementing materials. However, the method stated by ASTM E399: Linear-Elastic Plane-Strain Fracture Toughness $K_{IC}$ of Metallic Materials was found to be applicable to cement matrix (Li et al., 1995; ASTM Standard E399. 2003) and therefore used throughout the study.

Matrix specimens were kept in plastic bags at $95 \pm 5\%$ RH, $23 \pm 2$ $^{o}$C and toughness tests were performed (Figure 3.12) at the end of 7 and 28 days by using four beams on each specified date.

Figure 3.11 Fracture toughness test setup



Figure 3.12 Performance of fracture toughness test

During the tests, three-point bending loading was applied with the rate of 0.002 mm/s over purposely grooved 30 mm-notch on the specimens as it is prescribed by the specification and matrix toughness values of the specimens were calculated with the equation given below in accordance with following Equation (3.1):

$$K_Q = \frac{P_Q S}{B W^{\frac{3}{2}}} \cdot f\left(\frac{a}{W}\right) \qquad (3.1)$$

Where;

$P_Q$: Applied load,

$S$: Span width,

$B$: Height of the specimen,

$W$: Depth of the specimen, and

$f\left(\dfrac{a}{W}\right)$: geometric calibration factor (varying between 1.91 and 2.18 with respect to

determined exact depth of the specimens )

### 3.3.4 Autogenous Shrinkage

Linear prismatic molds, also called as shrinkage drains, were used while taking autogenous shrinkage measurements (Figure 3.13). The drains were composed of inner and outer molds. The inner mold, which was embedded inside the outer mold, measured 1000×60×90 mm.
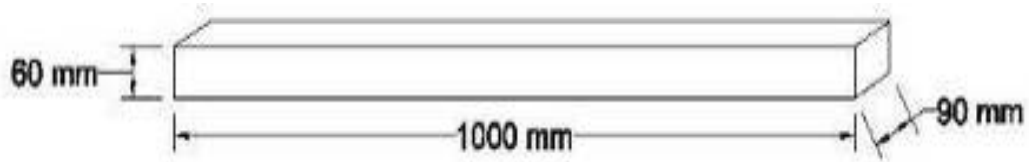


**(a) Inner mold**
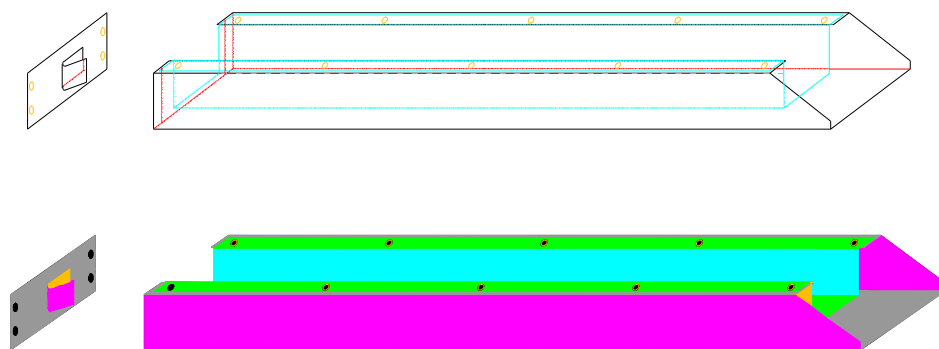


**(b)Outer mold and metal plate**



**(c) Mold, LVDT and spring bar**

Figure 3.13 Schematic illustration of autogenous shrinkage drain

In order to prevent friction inside the inner mold, the surfaces were covered with teflon sheets. The drains had two ends, one of which was closed and the other was free to move with an attached LVDT to measure instantaneous length changes in time. In addition to the LVDT, each drain had its own supplementary thermocouple placed between the inner and outer molds to measure temperature changes. Before placing fresh mixtures inside the drains, aerosol teflon was sprayed over the teflon cover and the inner mold of the drains was completely covered with stretch wrap (see Figure 3.14).



(a)          (b)

Figure 3.14 View of autogenous shrinkage test set-up a) during the preparation b) during the autogenous shrinkage test

This was done so mixtures were entirely isolated from the environment to better investigate the sole influence of hydration processes on autogenous shrinkage of HES-ECCs. Once the placement of fresh mixtures was completed, the top surface of the drains was covered with previously placed stretch wrap and an additional teflon sheet. LVDT measurements were started after the setting time of the mixtures was reached; until this time only temperature changes were recorded. Since it is not always easy to estimate the time needed for different mixtures to set, a common time interval was used for all mixtures. The time needed for LVDT measurements to begin was based on the period in which maximum heat liberation was observed, which worked out to two hours for all mixtures. All of the drains were kept in laboratory conditions at 23±2 $^{\circ}$C, and 50±5% RH. The changes in LVDT and temperature measurements were recorded by a data acquisition system every 10 minutes for one week.

## 3.3.5 Drying Shrinkage

Three 285×25×25 mm (11.2×1.0×1.0 in) bar specimens (see Figure 3.15) were also cast for each mixture to determine drying shrinkage up to 90 days after an initial curing of one day in the mold. During the production of the bars, gauge studs were placed into the molds coaxially and the mixtures were then poured. For each type of mixture, three bar specimens were prepared and stored in the laboratory at 23±2 °C and 50±5% RH until pre-determined testing ages.



Figure 3.15 Drying shrinkage device and samples

# CHAPTER 4

# RESULTS AND DISCUSSIONS

## 4.1 Compressive Strength

The compressive strength test results obtained from HES-ECC mixtures (in accordance with ASTM C39) are presented in Table 4.1. Each piece of data given in the table is the average of six cubic specimens. The factors affecting compressive strength development in the mixtures include binder type, W/CM ratio, the type of chemical admixture used and dosage. Therefore, depending on these parameters, the results varied substantially. As shown in Table 4.1, at the end of six hours, HES-ECC_2 control specimens had the highest compressive strength value with 33.6 MPa. In the HES-ECC_1 and HES-ECC_3 specimens, these values were 26.9 MPa and 29.6 MPa, respectively. The results showed an increasing trend up to 28 days, regardless of mixture type. Escalation in compressive strength results, however, was more visible until the end of 24 hours, since hydration reactions slowed down beyond this time period. When the results obtained from the HES-ECC_1 and HES-ECC_2 mixtures are compared, the effect of S/PC ratio on compressive strength at the end of six hours can be seen more clearly.

At the same W/CM ratio, as S/PC ratio decreased from 0.84 to 0.60, an almost 25% increase in the compressive strength of control specimens was monitored. The probable reason for this behavior is the higher amount of tricalcium silicate ($C_3S$) and tricalcium aluminate ($C_3A$), which are mainly responsible for calcium silicate hydrate (C-S-H) gel formation. Another reason for increased compressive strength with lower S/PC ratio could be the finer particle size of CEM I 52.5R Portland cement (460 $m^2$/kg) compared to slag (425 $m^2$/kg). When the number of finer particles in the mixtures increased, the pores in the cementitious matrix filled better, leading to denser microstructure and higher compressive strength results.

Table 4.1. Mechanical properties of HES-ECC mixtures

| Mixture ID | | Compressive strength (MPa) | | | | Flexural strength (MPa) | | | | Mid-span beam deflection (mm) | | | | Fracture toughness (MPa×m$^{1/2}$) | |
|---|---|---|---|---|---|---|---|---|---|---|---|---|---|---|---|
| | | 6 h. | 24 h. | 7 d. | 28 d. | 6 h. | 24 h. | 7 d. | 28 d. | 6 h. | 24 h. | 7 d. | 28 d. | 7 d. | 28 d. |
| HES-ECC_1 | **Control** | 26.9 | 64.4 | 85.0 | 95.1 | 8.0 | 9.5 | 10.9 | 11.1 | 3.6 | 2.7 | 1.4 | 1.0 | 0.93 | 1.03 |
| | **C_25%** | 23.3 | 52.8 | 73.9 | 80.7 | 8.0 | 9.1 | 10.6 | 11.7 | 3.4 | 3.0 | 2.7 | 2.4 | 0.79 | 0.88 |
| | **C_50%** | 20.7 | 41.9 | 68.6 | 76.0 | 7.8 | 9.0 | 10.1 | 11.0 | 3.4 | 2.9 | 2.5 | 2.3 | 0.65 | 0.72 |
| | **F_25%** | 26.2 | 58.6 | 81.5 | 88.0 | 8.1 | 9.5 | 10.8 | 11.4 | 3.8 | 3.2 | 2.5 | 2.3 | 0.81 | 0.90 |
| | **F_50%** | 22.0 | 47.2 | 73.9 | 82.5 | 7.9 | 8.9 | 10.1 | 11.3 | 3.7 | 3.3 | 2.6 | 2.4 | 0.68 | 0.75 |
| HES-ECC_2 | **Control** | 33.6 | 68.4 | 84.8 | 93.0 | 8.7 | 10.0 | 11.0 | 12.5 | 2.8 | 2.0 | 1.4 | 1.2 | 1.0 | 1.1 |
| | **C_25%** | 29.7 | 60.8 | 76.5 | 84.0 | 8.6 | 9.6 | 11.0 | 12.2 | 3.1 | 2.4 | 2.2 | 1.9 | 0.82 | 0.90 |
| | **C_50%** | 27.9 | 44.8 | 62.8 | 74.3 | 7.4 | 9.1 | 10.2 | 11.3 | 2.9 | 2.5 | 2.3 | 2.0 | 0.73 | 0.81 |
| | **F_25%** | 32.0 | 62.3 | 78.6 | 90.0 | 8.8 | 9.7 | 10.3 | 11.9 | 3.5 | 2.9 | 2.2 | 2.2 | 0.84 | 0.90 |
| | **F_50%** | 28.3 | 51.3 | 67.7 | 78.4 | 7.8 | 9.1 | 9.5 | 11.5 | 3.7 | 3.1 | 2.4 | 2.2 | 0.77 | 0.85 |
| HES-ECC_3 | **Control** | 29.6 | 56.2 | 64.6 | 75.7 | 7.2 | 8.6 | 10.0 | 10.2 | 2.3 | 1.9 | 1.2 | 1.0 | 0.89 | 0.93 |
| | **C_25%** | 25.2 | 38.8 | 52.7 | 59.6 | 6.7 | 8.3 | 9.1 | 10.0 | 2.4 | 2.0 | 1.6 | 1.5 | 0.75 | 0.81 |
| | **C_50%** | 17.0 | 34.3 | 42.6 | 47.4 | 6.0 | 6.2 | 8.9 | 9.3 | 2.3 | 2.3 | 2.2 | 1.5 | 0.62 | 0.71 |
| | **F_25%** | 27.6 | 43.9 | 54.9 | 63.2 | 6.9 | 8.2 | 9.6 | 9.8 | 2.9 | 2.5 | 2.4 | 2.0 | 0.76 | 0.85 |
| | **F_50%** | 19.0 | 36.5 | 47.1 | 51.2 | 6.2 | 6.9 | 8.6 | 9.5 | 3.4 | 2.9 | 2.4 | 2.2 | 0.66 | 0.73 |

Along with the filler effect, the higher fineness and particle surface area of Portland cement provide more nucleating sites and OH− ions as well as alkalis into the pore fluid (Li and Zhao, 2003). When six-hour compressive strength results of HES-ECC_2 and HES-ECC_3 mixtures are compared, it can be concluded that W/CM is a better criterion in defining the changes. Despite the significant drop in S/PC ratio (from 0.60 to 0.00), a slight increase in W/CM ratio (from 0.23 to 0.34) caused almost 12% of the overall decrease in the results.

Although lightweight perlite aggregate is much weaker than the silica sand it replaces, specimens with LWA are expected to produce higher strength due to internal curing and enhanced hydration considerations (Lura, et al., 2004). However, as seen in Table 4.1, an increase in the LWA amount caused a significant decrease in compressive strength, irrespective of replacement level. For example, replacement with 25% coarse LWA caused a 14% decrease in six-hour compressive strength value of HES-ECC_1 mixture. At a 50% replacement level, the loss increased to 23%. However, the decreasing trend was less pronounced in the case of fine LWA replacement levels; a 3% and 20% decrease was monitored with 25% and 50% fine LWA replacement, respectively. During the production of ECC, it is desirable to work with finer aggregates, since uniform distribution of fibers is vital for superior material characteristics. With coarser LWA usage, the formation of fiber bundles – which behave as voids in the cementitious matrix – occurs more easily. The reason for reduced compressive strength results with the addition of LWA may therefore be related to non-uniform fiber distribution and balling of fibers. It can also be correlated with the increase in stress concentrations over coarse aggregates upon loading, since the larger the aggregate size, the higher the local water-cement ratio in the interfacial transition zone and, consequently, the weaker the concrete (Mehta and Monteiro, 2006). Despite variations observed in the results, the minimum compressive strength limit (20 MPa) set throughout the study was satisfied by all mixtures at the end of six hours, excluding those obtained from HES-ECC_3 specimens at 50% pre-soaked LWA replacement level.

## 4.2 Flexural Strength (Modulus of Rupture-MOR)

While uniaxial tensile tests are considered to be the most accurate method of assessing the flexural performance of a composite, they are seldom carried out,

mainly because the specimen holding devices introduce secondary stresses that cannot be ignored (Mehta and Monteiro, 2006). Flexural strength testing of ECC is also an indirect measure of direct tensile performance, since flexural-hardening behavior stands as one of the most important features of ECC. Previous studies have demonstrated that deflection capacity obtained from flexural strength tests can be correlated back to tensile strain capacity in an almost linear manner, as long as the material is qualified as truly strain hardening (Qian and Li, 2007 and Qian and Li, 2008). Therefore, throughout this study, four-point bending testing was used to investigate flexural strength and ductility by measuring mid-span beam deflection capacity of HES-ECC mixtures.

Table 4.1 tabulates the flexural strength test results of different HES-ECC mixtures. Each piece of data presented in the table was calculated by taking the average of six prismatic specimens. As seen in the table, HES-ECC_2 control specimens (without pre-soaked LWA) showed the highest flexural strength attainment with 8.7 MPa flexural strength at the end of six hours. The HES-ECC_2 mixture was followed by HES-ECC_1 and HES-ECC_3 control mixtures with 8.0 and 7.2 MPa, respectively. The increase in MOR values with time was not as drastic as it was in the compressive strength results; HES-ECC_1, HES-ECC_2 and HES-ECC_3 mixtures achieved only 3.1, 3.8 and 3.1 MPa of enhancement between six hours and 28 days of age, respectively. Although W/CM and S/PC ratios are two important parameters in realizing flexural strength development, relatively low increments in flexural strength results were observed with time compared to compressive strength. This trend can be attributed to more complex material properties that can significantly affect MOR values such as tensile strain capacity, tensile first cracking strength, and ultimate tensile strength (Qian and Zhou, et. al. 2009). Although the usage of pre-soaked LWA caused minor enhancements in MOR values in some of the specimens at the end of six hours, it is clear that incorporation of LWA into the mixtures resulted in an overall decrease in MOR values at any specified age. As the amount of pre-soaked LWA was increased from 25% to 50%, the drop in MOR values became more evident. For example, in the case of HES-ECC_3 control specimens, while the average MOR value was found to be 7.2 MPa at the end of six hours, it dropped to 6.9 MPa and 6.2 MPa with 25% and 50% fine LWA replacement, respectively. The decreasing trend was even more pronounced with coarse LWA usage; with the

inclusion of 25% and 50% of coarse LWA, MOR values decreased to 6.7 MPa and 6.0 MPa , respectively. The reduced strengths with increased LWA replacement level may be due to non-uniform distribution of fibers. The addition of significantly coarser LWA (compared with silica sand) encourages the balling of fibers. Due to inadequate coating of fibers by the matrix, fiber-to-matrix bonding is reduced, which in turn causes decreased flexural load carrying capacity. According to NJDOT, the minimum flexural strength of fast track concrete for repair purposes should be 2.4 MPa in six hours (FHWA, 1999). The California State Department of Transportation (Caltrans) requires 2.8 MPa of flexural strength attainment in four hours before putting the pavement repair into service (Qian and Zhou, et. al. 2009). It therefore appears that despite the decreases in MOR results with addition of LWA, the lowest value obtained from all HES-ECC mixtures (HES-ECC_3 with 50% of coarse LWA replacement, 6.0 MPa) was more than enough to satisfy the minimum requirements of different authorities for a repair material.

## 4.3 Mid-Span Beam Deflection

Mid-span beam deflection values, which reflect HES-ECC ductility, are presented in Table 4.1. As seen from the table, results varied significantly depending on mixture proportion, LWA replacement and curing time. When the deflection values of HES-ECC_1 and HES-ECC_2 mixtures are considered, specimens with lower S/PC ratio (HES-ECC_2 mixtures) at the same W/CM ratio exhibited lower deflection values in general. According to the micromechanical model of steady state cracking, which is essential for achieving strain hardening behavior, high matrix fracture toughness reduces the margin to obtain multiple microcracking behavior (Li, 1995). The decreased deflection values in the HES-ECC_2 specimens compared with the other mixtures could be due to higher fracture toughness, bond strength and friction between the HES-ECC_2 matrix and the fibers (please see Fracture Toughness section). The overall deflection results of all mixtures show that the lowest values were obtained from the mixture with the highest W/CM ratio (HES-ECC_3). This finding is not in agreement with Yang et al. (Yang et al.,2010.), who studied the effects of W/CM ratios ranging from 0.25 to 0.37 on the properties of ECC and concluded that the higher the W/CM ratio, the higher the flexural deflection capacity. The reason behind this behavior becomes clear in Table 3.3. Despite the significant

increase in W/CM ratio, there was no slag incorporated in the HES-ECC_3 mixtures. This led to higher amounts of cement content but also caused a substantial increase in the amount of sand, which is notably coarser than slag. Therefore, it is likely that the uniform distribution of fibers was interrupted due to coarser aggregate gradation in the HES-ECC_3 mixture, leading to insufficient coating of individual fibers by matrix, and thus a reduction in bonding between fiber and matrix, which is an important factor influencing ductility (Soroushian et al.,1992.). As shown in Table 4.1, as curing time was extended, a decreasing trend in deflection values of the mixtures occurred regardless of LWA usage. For example, while the average deflection value of the HES-ECC_1 control mixture at the end of six hours was 3.6 mm , this value decreased to 2.7 mm, 1.4 mm and 1.0 mm at the end of 24 hours, 7 days and 28 days, respectively. Reduction in mid-span beam deflection values with time is highly attributable to the continuous evolution of matrix and fiber/matrix interface properties and is expected to be limited as the matrix maturity is stabilized.

The usage of saturated LWA was also found to be influential on deflection values, as seen in Table 4.1. Increase in saturated LWA amount in the mixtures positively affected the mid-span beam deflection results. For instance, at the end of 28 days, HES-ECC_1 control specimens showed a deflection value of 1.0 mm while inclusion of 25% and 50% saturated coarse LWA increased it to 2.4 mm and 2.3 mm, respectively. Replacement of saturated fine LWA was also found to be as effective on deflection results as coarse LWA; 1.0 mm deflection value increased to 2.3 mm and 2.4 mm as replacement rates reached 25% and 50% levels. The ductility of ECC material is dependent not only on fiber effectiveness in transferring stress back into the matrix, but also on the toughness of the matrix itself (Li, 1997). Therefore, the increase in deflection results with different LWA replacements may be better understood by taking toughness results into consideration. Table 4.1 shows that toughness is reduced with the incorporation of saturated LWA, which means that the occurrence of multiple micro-cracks instead of localized cracks with larger crack widths was triggered in favor of attaining large deformability.

Another striking outcome of the deflection tests is that specimens with fine LWAs showed increased deflection values compared to specimens with coarse LWAs. For example, the HES-ECC_3 specimens with 25% of coarse LWA replacement showed

deflection capacity of 2.4 mm at the end of six hours, while the value was 2.9 mm for specimens incorporating 25% fine LWA. Moreover, the increasing trend became more evident as LWA replacement level was increased to 50%. While 2.3 mm of deflection was monitored for the same specimens with 50% coarse LWA replacement in six hours, the result increased to 3.4 mm with 50% fine LWA. The specimens exhibited similar results regardless of the mixture type and curing time. The reason for the negative effects of increasing aggregate size on ductility has already been discussed earlier in this section.

## 4.4 Fracture Toughness

Toughness tests were conducted on prismatic mortar specimens at the ages of seven and 28 days; the results are shown in Table 4.1. Each piece of data displayed in Table 4.1 was found by averaging the results of at least five specimens. As seen from the table, HES-ECC_2 specimens exhibited the highest toughness results with values ranging between 0.96 and 0.73 MPa$\times$m$^{1/2}$ at the end of seven days. The same modality was also observed for the results obtained at the end of 28 days. In addition, HES-ECC_3 specimens resulted in the lowest results at the end of any specified time. When the fracture toughness test results of matrices (ECC without PVA fiber) are carefully evaluated, a close relationship between toughness and compressive strength is evident, since both parameters are markedly affected by the changes occurring in matrix maturity with time. The addition of saturated LWA was expected to increase the toughness results, since it was believed that internally available water inside the LWAs would trigger further hydration reactions at a very low W/CM ratio, leading to enhanced matrix maturity and matrix fracture toughness results. However, as also seen from Table 4.1, the overall toughness results differ from the expectation since LWA replacement resulted in a 15 to 30% reduction in toughness values of seven-day cured HES-ECC specimens. This drop is most probably due to the higher porosity of matrices with the inclusion of LWAs, since expanded perlite is much weaker and coarser than the silica sand it replaces (Figure 3.5).
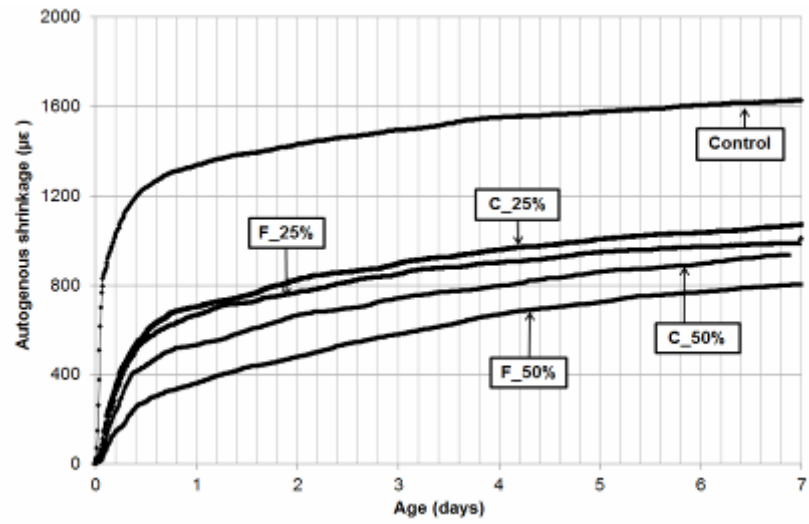
## 4.5 Autogenous Shrinkage

Concretes with very low W/CM ratio suffer from increased autogenous shrinkage, which is caused by self-desiccation of the cementitious matrix. As previously

mentioned, the primary goal during the production of the HES-ECC mixtures was the attainment of adequate compressive strength, especially at early ages, which could substantially contribute to the faster consumption of readily available mix water. Thus, autogenous shrinkage caused by self-desiccation of the matrix must be controlled. According to reports, conventional curing procedures are not sufficient to eliminate autogenous shrinkage in concrete due to the restrictions of matrix tightness on the water transportation (Bentz and Snyder, 1999). For this reason, the production of HES-ECC mixtures involved a proven technique to minimize autogenous shrinkage strains where pre-soaked LWAs are used as internal curing agents.

Figure 4.1, autogenous shrinkage of HES-ECC mixtures measured from two hours after mixing up to one week as a function of age. As seen from the figure, all mixtures except HES-ECC_3 mixtures with LWA show an increase in the results with time, regardless of mixture type. This trend, which is directly related to the acceleration of hydration reactions and self-desiccation of the cementitious matrix, was found to be quite reasonable. It is also important to note that for all mixtures, most of the autogenous shrinkage strains were developed until the end of one day. Therefore, during the design of HES-ECC structures, one must take into account that proposed techniques to prevent self-desiccation and early age cracking should be effective for at least one day after mixing.

As evident from Figure 4.1, the highest autogenous shrinkage development at the end of seven days was exhibited by the HES-ECC_1 control mixture with 1627 $\mu\varepsilon$. This value decreased to 1471 $\mu\varepsilon$ and 706 $\mu\varepsilon$ for HES-ECC_2 and HES-ECC_3, respectively. The changes in the results were not drastic and started to stabilize beyond one day as the hydration reactions start to slow down. In the HES-ECC_3 control mixture, the lower autogenous shrinkage values were found to be closely related to the higher W/CM ratio, which is in good correlation with the literature (Tazawa and Miyazawa, 1993), (Brooks, Cabrera, Megatjohari, 1998) , (Mak, Ritchie, Taylor and Diggins, 1998) and (Persson, 1998).. Since autogenous shrinkage is the result of water consumption due to cement hydration, the greater free water content results in less autogenous shrinkage.

**(a) HES-ECC  1**
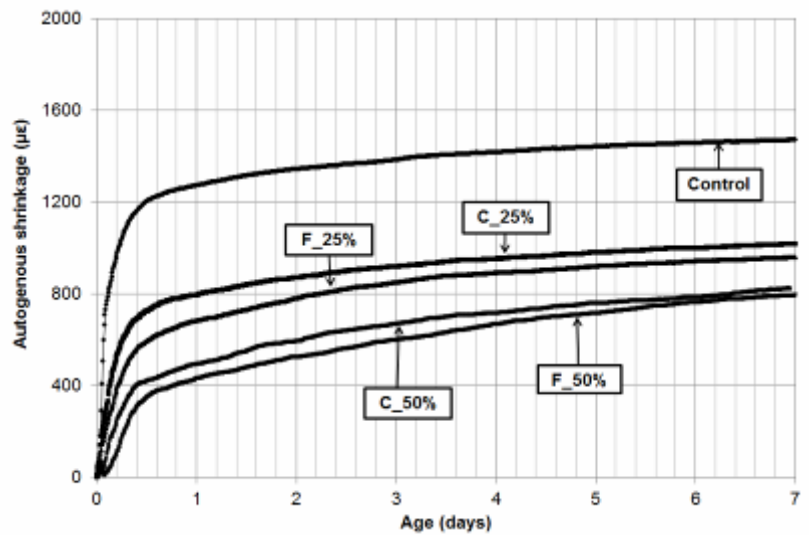


**(b) HES-ECC_2**
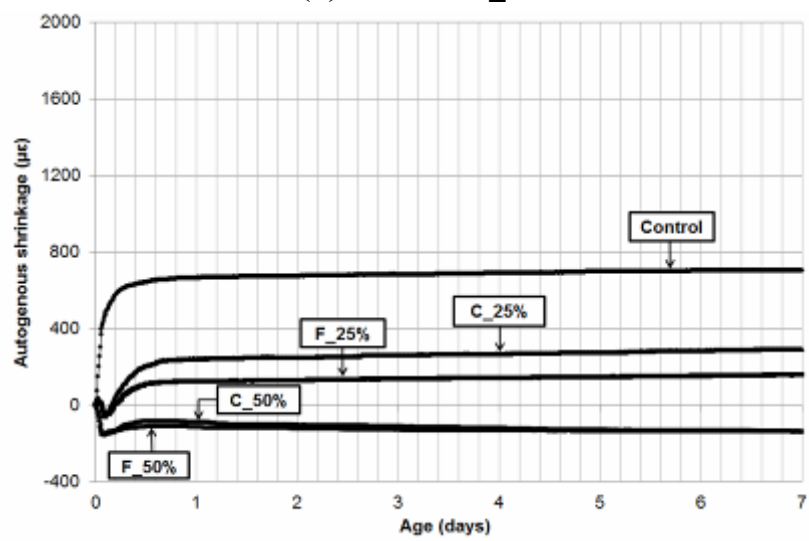


**(c) HES-ECC_3**

Figure 4.1 Autogenous shrinkage of HES-ECC mixtures

The lower autogenous shrinkage of the HES-ECC_3 control specimens can also be attributed to the substantial decrease in cementitious materials content (cement + slag) and the increase in aggregate content, both of which significantly affect hydration reactions, restrained effect and self-desiccation (see Table 3.3).

The addition of pre-soaked LWAs into HES-ECC mixtures caused significant changes in autogenous shrinkage results. For example, replacement with 25% coarse LWA caused a 34% decrease in autogenous shrinkage of the HES-ECC_1 control specimens. This value increased to 38% with fine LWA usage. As the pre-soaked LWA replacement level was increased to 50%, the decreasing trend became even more evident, with 43% and 51% reductions observed for coarse and fine LWAs, respectively. The same modality was monitored for the rest of the mixtures as well. Specimens with fine LWAs may show higher reduction in autogenous shrinkage results due to more uniform distribution of the aggregates in the cementitious matrix. The effectiveness of internal curing through pre-soaked LWA usage is significantly affected by the particle size and water absorption capacity of the aggregate used. It has been reported that the small particle size and coarse pore structure of LWA achieve optimum internal curing (Zhutovsky, Kovler and Bentur, 2002). Therefore, the explanation for lower autogenous shrinkage results with fine LWA could be that the spacing among the LWAs was reduced due to better distribution of finer particles, making paste volume more accessible to the water in the internal reservoirs. It is important to note that in order to prevent self-desiccation of the matrix, the diffusion of water from the LWAs into the matrix must be as fast as possible, since the transportation of water slows as the paste gets stiffer, especially in the case of early-stiffening HES-ECC mixtures. Although coarse LWAs can absorb more water (144%) compared to fine LWAs (131%), the results are surprising in that HES-ECC specimens with coarse LWAs showed higher autogenous shrinkage strains after seven days. This discrepancy indicates that it is not the total water amount retained in LWA pores that is the best parameter of internal curing efficiency, but the fact that the water is effectively used to neutralize self-desiccation.

The effectiveness of pre-soaked LWAs in mitigating autogenous shrinkage can be best detected by checking the autogenous strain development in the HES-ECC_3 mixture. When the data presented in Figure 4.1 were evaluated, it was clear that

LWA replacement, regardless of size and quantity, was much more efficient for HES-ECC_3 than for other mixtures. Figure 4.1 also shows that the addition of 25% coarse and fine LWA into the mixtures substantially minimized strain development due to self-desiccation, so that autogenous strain developments after seven days were only 293 $\mu\varepsilon$ and 159 $\mu\varepsilon$ for coarse and fine LWA additions, respectively. It is also clear from Figure 4.1 that for a very limited time, the curves of these specimens went down to the negative portion of the graph, implying swelling of the pastes and the occurrence of beneficial compressive stresses. According to Cusson and Hoogeveen (Cusson and Hoogeveen, 2008), since concrete material is quite weak in tension at the very beginning of setting, the risk of cracking must be considered when compressive stresses caused by paste expansion start to turn into tensile stresses due to contraction. Therefore, as long as stresses are kept in the compression zone, autogenous shrinkage strains can be minimized or even terminated completely. Expansion observed in the HES-ECC_3 specimens incorporating 50% coarse and fine LWA correspond the abovementioned modality, with -155 $\mu\varepsilon$ and -159 $\mu\varepsilon$, respectively. This shows that all of the stresses caused due to expansion in these specimens were in compression and not damaging in terms of crack occurrence. One must note that this behavior of the HES-ECC_3 mixtures with 50% LWA is one of most important criteria for obtaining truly resilient repair materials; it may lead to the realization of totally crack-free materials with the characteristics of high early strength and high deformability.
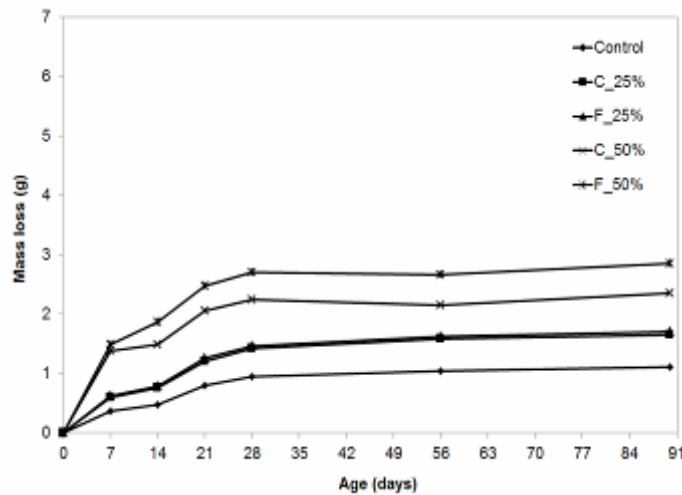
## 4.6 Drying Shrinkage

Figures 4.2, 4.3 and 4.4 show the drying shrinkage results of HES-ECC mixtures. The results were calculated by taking the average of three bar specimens kept in laboratory conditions at 23±2°C, and 50±5% RH until pre-determined testing ages. As seen from Figures 4.2 (a), 4.3 (a) and 4.4 (a), the drying shrinkage results varied significantly depending on the curing time and pre-soaked LWA usage. The drying shrinkage results obtained at the end of 90 days ranged between 984 and 1202 $\mu\varepsilon$ for HES-ECC_1 specimens, 1194 and 1348 $\mu\varepsilon$ for HES-ECC_2 specimens and 1061 and 1201 $\mu\varepsilon$ for HES-ECC_3 specimens, respectively. It is important to note that most of the drying shrinkage strains developed within seven days and the results started to stabilize after 28 days. When the drying shrinkage results of different HES-ECC control mixtures are compared, it can be seen that HES-ECC_3 specimens showed

the lowest strain development almost at the end of each test period. The probable reasons for this trend are the relatively low binder and increased sand amount in the HES-ECC_3 mixtures. It is widely known that in a cementitious system, the paste tends to shrink while aggregates resist contraction.
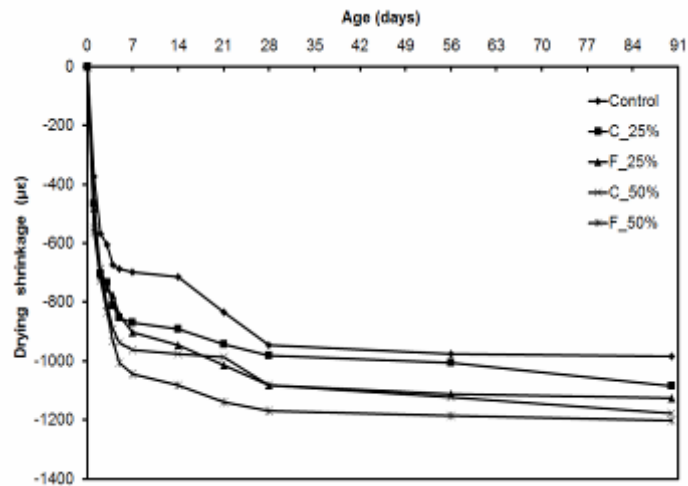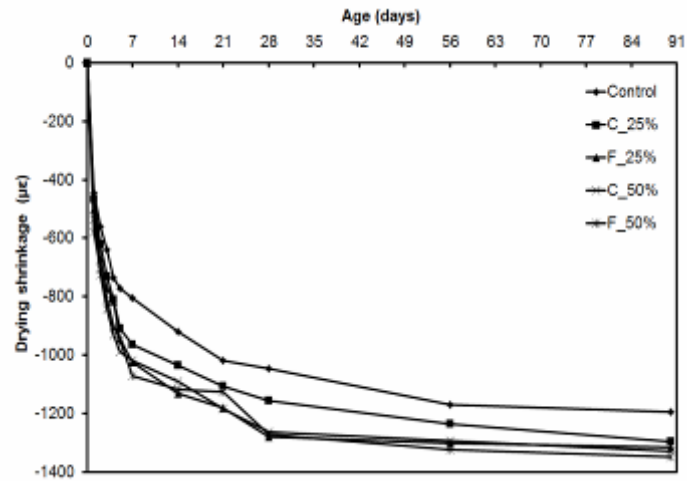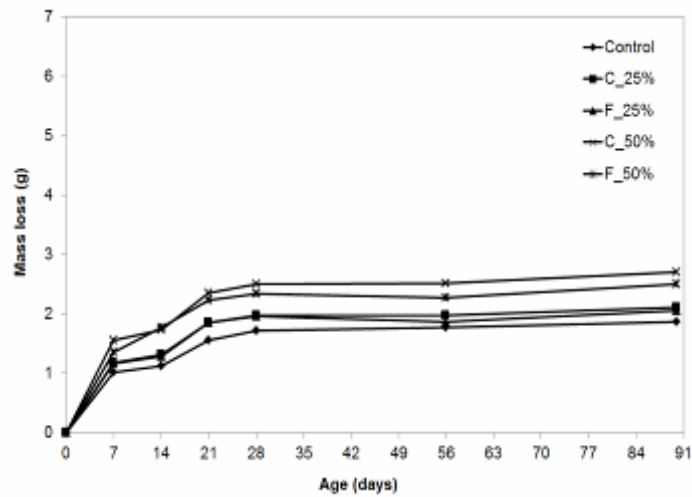


**(a) HES-ECC_1**



**(b) HES-ECC_1**

Figure 4.2 (a) Drying shrinkage and (b) mass loss of HES-ECC_1

Therefore, reductions in binder amount can decrease the overall shrinkage caused by drying. Although its effect was limited due to small grain size, increased sand amount contributed to the reductions in drying shrinkage of the HES-ECC_3 mixtures.

**(a) HES-ECC_2**



**(b) HES-ECC_2**

Figure 4.3 (a) Drying shrinkage and (b) mass loss of HES-ECC_2

Incorporating pre-soaked LWAs into concrete mixtures caused an increase in drying shrinkage results. For example, at the end of one day, 25% coarse and fine LWA replacement led the results of the HES-ECC_1 control specimens to increase by 25% and 29%, respectively. When the LWA usage was increased to 50%, contraction due to drying became much more apparent with increased of 46% and 50%. According to Zhang et al. (Zhang, Li and Paramasivum, 2005), the drying shrinkages of normal weight and lightweight aggregate concretes would be similar, and when exposed to drying, LWA containing concrete would exhibit lower shrinkage due to its lower autogenous shrinkage. Higher drying shrinkage results with the incorporation of pre-

soaked LWAs may be attributed to greater water loss from concrete upon drying, which in turn causes a higher increase in drying shrinkage results. This observation was also confirmed from mass loss results as shown in Figures 4.2 (b), 4.3 (b) and 4.4 (b).
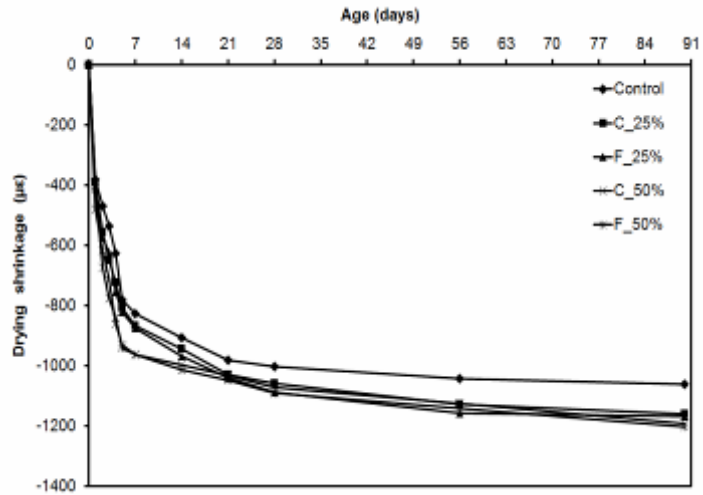


**(a) HES-ECC_3**
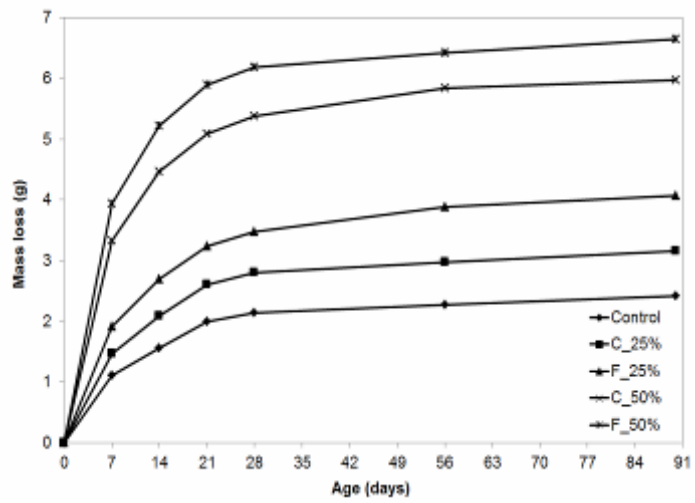


**(b) HES-ECC_3**

Figure 4.4 (a) Drying shrinkage and (b) mass loss of HES-ECC_3

# CHAPTER 5

## CONCLUSIONS

In this study, composites incorporating high volumes of slag with the characteristics of high early strength, high deformability and superior dimensional stability were developed. HES-ECC mixtures with two different W/CM (0.23 and 0.34) and S/PC (0.60 and 0.84) were produced. During the production, coarse (with MAS of 4 mm) and fine (with MAS of 2 mm) pre-soaked LWAs were substituted with silica sand at fractions of 25% and 50% by volume in order to take advantage of the dual efficiency of LWAs on ductility and early age cracking. Control specimens with no LWA replacement were also produced for comparison purposes. Mechanical properties, compressive strength, flexural strength, mid-span beam deflection and fracture toughness properties were evaluated, dimensional stability properties, autogenous shrinkage properties of HES-ECC mixtures were investigated, and the following results were drawn:

1. Although the compressive strength results were strongly influenced by the changes in W/CM, S/PC and pre-soaked LWA incorporation levels, the HES-ECC mixtures produced in this study (with the exception of HES-ECC_3 specimens with 50% of LWA replacements) satisfy the minimum compressive strength value of 20 MPa in six hours. The minimum flexural strength value obtained from the mixtures was found to be 6 MPa or higher at the end of six hours, which is far beyond from the minimum values set by different authorities (FHWA, Manual of Practice, 2001). These results show that the repair materials made with the HES-ECC mixtures designed in this study can effectively be returned to service in six hours or less without compromising strength requirements.

2. The minimum flexural deflection capacity was obtained from the HES-ECC control specimens with 2.3 mm (0.09 in) in six hours. Although this value is regarded

as a minimum, it accounts for nearly 100 times higher deflection capacity under four point loading compared to that of conventional concrete repairs. This increased ductility under bending is strongly related to reduction in matrix toughness and the effectiveness of fibers in transferring stresses. The superior ductility of HES-ECC specimens upon bending is an indispensable material property in the realization of durable repairs.

3. Although some of the mixtures have triggered increments in autogenous shrinkage strains (especially control specimens), addition of pre-soaked LWAs effectively minimized self-desiccation. Moreover, autogenous shrinkage results of the HES-ECC_3 mixtures with 50% pre-soaked LWAs show that with proper adjustments, concrete repairs that are truly resistant to cracks occurring due to self-desiccation can be produced with sufficient mechanical properties.

# REFERENCES

ACI Committee 116R. (1994). Cement and concrete terminology. ACI manual of concrete practice.

ACI Committee 212. (1963). Admixtures for concrete. ACI Journal Proceedings 60 (11):1481-524.

ACI Committee 224R. (2001). Control of cracking in concrete structures. American Concrete Institute, Farmington Hills, Michigan.

ACI Committee 318R (2002). Building code requirements for structural concrete and commentary. American Concrete Institute, Farmington Hills, Michigan, pp. 443.

Alhassan, Muhammad A. (2007). Performance-based aspects and structural behavior of high performance fibrous bonded concrete overlays, PhDThesis.

ASTM Standard C39. (2003). Standard test method for compressive strength of cylindrical concrete specimens. American Society for Testing and Materials. West Conshohocken, PA, USA.

ASTM Standard C157. (2004). Test method for length change of hardened hydraulic cement mortar and concrete. American Society for Testing and Materials. West Conshohocken, PA, USA.

ASTM Standard C 666. (1991). Standard test method for resistance of concrete to rapid freezing and thawing. American Society for Testing and Materials, Philadelphia, USA.

ASTM Standard C 672. (2001). Standard test method scaling resistance of concrete surfaces exposed to de-icing chemicals. American Society for Testing and Materials, Philadelphia, USA.

ASTM Standard C989. (2009). Standard specification for slag cement for use in concrete and mortars. American Society for Testing and Materials. West Conshohocken, PA, USA.

ASTM Standard E399. (2003). Test method for plane-strain fracture toughness of metallic materials. American Society for Testing and Materials. West Conshohocken, PA, USA.

ASTM Standard C1260. (1994). Standard test method for potential alkali reactivity of aggregates (Mortar-bar method). In: Annual book of American Society for Testing and Materials, Philadelphia, USA.

American Association of State Highway and Transportation Officials. (2002) The bottom line, AASHTO, Washington, D.C., USA, pp.1-5.

D.P. Bentz and K.A. Snyder (1999). Protected paste volume in concrete – Extension to internal curing using saturated lightweight fine aggregate, *Cement and Concrete Research*, **29** (11) 1863-1867.

E. Tazawa and S. Miyazawa (1993). Autogenous shrinkage of concrete and its importance in concrete technolog, in: Z.P. Bazant, L. Carol (Eds.), Creep and Shrinkage of Concrete , *Proceedings of the 5th International RILEM Symposium*, E & FN Spon, London, pp. 159–168.

Edmeades, R. M. and Hewlett, P. C. (1992) Cement admixtures, Lea's chemistry of cement and concrete, 4th ed., ed. P. C. Hewlett, Arnold, London, pp. 837-902.

Federal Highway Administration (FHWA). (2001). Paving repair finds a four-hour champion, *Concrete Construction*, 46 (**12**) 69-70. FHWA, Manual of Practice:

Materials and Procedures for Rapid Repair of Partial-Depth Spalls in Concrete Pavements, 135 pp.

Ferraris, C. F. and Lobo, C. (1998). Processing of HPC. *Concrete International,* **20** (4) 61-64.

Frangopol, D. M. and Furuta, H. (2001). Proceedings of the US-Japan Workshop Life-cycle cost analysis and design of civil infrastructure systems. Reston, Virginia: ASCE.

Gustavo J.Parra-Montesinos. (2009). High-performance fiber reinforced concrete for highly damage-tolerant earthquake-resistant structures. University of Michigan Department of Civil and Environmental Engineering, USA.

Hewlett, P. C. and Young, J. F. (1989). Physico-chemical Interactions between ChemicalAdmixtures and Portland Cement. *Materials Education*, 9 (**4**) 389-433.

J. J. Brooks, J. G. Cabrera and M.A. MegatJohari. (1998). Factors affecting the autogenous shrinkage of silica fume high-strength concrete, in: E. Tazawa (Ed.), *Proceedings of International Workshop on Autogenous Shrinkage of Concrete*, Hiroshima, Japan, E & FN Spon,pp. 195– 201.

Knofel, D. and Wang, J. F. (1994). Properties of three newly developed quick cements. *Cement and Concrete Research*, 24 (**5**) 801-812.

Kong, J. H., Bike, S. and Li, V.C. (2003). Development of a self-consolidating engineered cementitious composite employing electrosteric dispersion/stabilization. *Cement and Concrete Composites*, Vol. 25, No.3, pp. 301-309.

Kunieda, M. and Rokugo, K. (2006). Recent progress on HPFRCC in Japan. *Advanced Concrete Technology*, **4,** 19-33.

Kurtz, S. Balaguru, P., Consolazio, G. and Maher, A. (1997). Fast track concrete for construction repair, Report No. FHWA 2001-015, New Jersey Department of Transportation, Trenton, N.J., 67 pp.

Li, V. C., Mishra, D. K. and Wu, H. C. (1995). Matrix design for pseudo strain-hardening fiber reinforced cementitious composites. *Materials and Structures*, **28**, 586-595.

Li, V. C. (1997). Engineered cementitious composites tailored composites through micromechanical modeling, in: N. Banthia, A. Bentur, A. Mufti (Eds.), Fiber Reinforced Concrete: Present and the Future, *Canadian Society for Civil Engineering*, pp. 64-97.

Li, V. C. (1997). Crack bridging in fiber reinforced cementitious composites with slip-hardening interfaces. *Mechanics and Physics of Solids,* **45**, 763-787.

Li, V. C., C. Wu, S. Wang, A. Ogawa and T. Saito (2002). Interface tailoring for strain-hardening PVA–ECC. *ACI Materials Journal,* **99** (5) 463–472.

Li, V. C. (2003). On engineered cementitious composites (ECC) a review of the material and its applications, *Advanced Concrete Technology*, **1**, 215-230.

Li, V. C., Horikoshi, T., Ogawa, A., Torigoe, S. and Saito, T. (2004). Micromechanics-based durability study of polyvinyl alcohol engineered cementitious composite (PVA-ECC). *ACI Materials Journal*, **101**, 242-248.

Li, V. C. (2005). Engineered Cementitious Composites. *Proceedings of ConMat'05*, Vancouver,Canada, August 22-24.

Li, V. C., Lepech, M. and Li, M. (2005). Final Report on Field Demonstration of Durable Link Slab for Jointless Bridge Decks Based on Strain-Hardening Cementitious Composites, submitted to Michigan Department of Transportation.

Li M. and Li V.C. (2011). High-early-strength engineered cementitious composites for fast, durable concrete repair—material properties. *ACI Materials Journal*, **108** (1) 3.

Lin, Z., Kanda, T. and Li, V.C. (1999), On interface property characterization and performance of fiber reinforced cementitious composites, *Concrete Science and Engineering*, **1**, 173-184.

Zhang, M. H., Li, L. and Paramasivum, P. (2005). Shrinkage of high-strength lightweight aggregate concrete exposed to dry environment. *ACI Materials Journal*, **102** (2) 86–92.

Malhotra, V. M., Berry, E. E., and Wheat, T. A. (1989), Superplasticizers in Concrete. *Proceedings of International Symposium*, Ottawa, (2 vols.), CANMET, Department of Energy, Mines and Resources, Ottawa, Canada, also published in part as ACI SP-62, American Concrete Institute, Detroit, MI.

Maruta, M., Kanda, T., Nagai, S.and Yamamoto, Y. (2005). New high-rise RC structure using pre-cast ECC coupling beam. *Concrete Journal*, **43,** 18-26.

Mather, B., and Warner, J., (2004). "Why do concrete repairs fail," interview held at University of Wisconsin, Department of Engineering Professional Development, site http://aec.engr.wisc.edu/resources/rsrc07.html.

Mays, G. (1992), Durability of Concrete Structures: Investigation, Repair, Protection.

Mehta P.K. and Monteiro P.J.M. (2006). Concrete: structure, properties, and materials. Third Edition, McGraw Hill, New York.

Miyazato, S. and Hiraishi, Y. (2005). Transport properties and steel corrosion in ductile fiber reinforced cement composites. *Proceedings of the Eleventh International Conference on Fracture*, Turin, Italy, March, pp. 20-25.

Naaman, A.E., and Reinhardt, H.W. (1996). Characterization of high performance fiber reinforced cement composites HPFRCC. *RILEM Proceedings* 31, Eds. A.E. Naaman and H.W. Reinhardt, 1-23.

Narayan, W. (2007). Infrastructure, climate change, sustainability: the challenge of design – strength or durability. *Concrete*, **41** (9) 31-33.

Neville, A. M. and Brooks, J. J. (1987), Concrete Technology, Longman Scientific andTechnical, 438 pages.

Nmai, C. K., Schlagbaum, T., and Violetta, B. (1998). A history of mid-range water reducing admixtures. *Concrete International*, **20** (4) 45-50.

Lura, P., Bentz, D. P., Lange, D. A., Kovler, K. and Bentur, A. (2004). Pumice aggregates for internal water curing. *PRO 36: Proceedings of the International RILEM Symposium on Concrete Science & Engineering - A Tribute to Arnon Bentur*, RILEM Publications S.A.R.L., pp. 137-151.

Parker, F. and Shoemaker, M. L. (1991). PCC pavement patching materials and procedures. *Materials in Civil Engineering*, **3** (1) 29-47.

Pyle, T. (2001). Personal communication on early strength concretes used in California, CALTRANS, USA.

Qian, S. and Li, V.C. (2007). Simplified inverse method for determining the tensile strain capacity of strain hardening cementitious composites. *Advanced Concrete Technology*, **5**, 235–46.

Qian, S., Zhou, J., De Rooij, M.R., Schlangen, E., Ye, G. and Van Breugel, K. (2009). Self-healing behavior of strain hardening cementitious composites incorporating local waste materials. *Cement and Concrete Composites*, **31**, 613–621.

Ramachandran, V. S. (1996). Concrete admixtures handbook, Noyes Publications, Park Ridge, NJ, USA

Ramachandran, V. S., Malhotra, V. M., Jolicoeur, C. and Spriato, N. (1987). Superplasticizer: properties and applications in concrete. Publ. No. MTL-14 (TR), CANMET National Resources Canada, Ottawa, Canada.

Rear, K., and Chin, D. (1990). Non-chloride, accelerating admixtures for early compressive strength. *Concrete International*, **12** (10) 55-58.

Rixom, M. R., and Mailvaganam, N. P. (1986). Chemical admixtures for concrete, 2nd ed., E & FN Spon, London.

Zhutovsky, S., Kovler, K. and Bentur, A. (2002). Efficiency of lightweight aggregates for internal curing of high strength concrete to eliminate autogenous shrinkage, *Materials and Structures*, **35** (2) 97-101.

Sarkar, S. L. and Wheller J. (2001).Microstructure development in an ultra- fine cement—part II. *Cement and Concrete Research,* 5 47–55.

Seehra, S. S., Gupta, S., and Kumar, S. (1993). Rapid setting magnesium phosphate cement for quick repair of concrete pavements – characterization and durability aspects. *Cement and Concrete Research*, **23** 2 254-266.

Soroushian, P., Nagi, M. and Hsu, J. (1992). Optimization of the use of lightweight aggregates in carbon fiber reinforced cement. *ACI Materials Journal*, 89, 267-276.

Sprinkel, M. M. (1991). Very-early-strength latex-modified concrete overlay. Report No. VTRC99-TAR3, Virginia Department of Transportation, Richmond, Virginia, 11pp.

Suthiwarapirak, P., Matsumoto, T. and Kanda, T. (2002). Flexural fatigue failure characteristics of an engineered cementitious composite and polymer cement mortars. *Materials, Concrete Structures and Pavements*, **718** (57) 121-134.

Şahmaran, M. and Li, V.C. (2007). De-icing salt scaling resistance of mechanically

loaded engineered cementitious composites. *Cement and Concrete Research*, 37, 1035-1046.

Şahmaran, M. and Li, V.C. (2009). Influence of microcracking on water absorption and sorptivity of ECC. *Materials and Structures*, **42** (5) 593-603.

Şahmaran, M. and Li, V.C. (2008). Durability of mechanically loaded Engineered Cementitious Composites under high alkaline environment. *Cement and Concrete Composites*, 30, 72-81.

Kojima, S., Sakat, N., Kanda, T. and Hiraishi, T. (2004). Application of direct sprayed ECC for retrofitting dam structure surface – application for Mitaka-Dam. *Concrete Journal,* **42** (5) 35-39 (In Japanese).

Turkish National Standards Institute TS EN 197-1 (2011;2012). Cement- Part 1: Compositions and conformity criteria for common cements.  Construction Sector Specialization Committee.

Turkish National Standards Institute TS EN 934-2 (2002). Admixtures for concrete, mortar and grout - Part 2: Concrete admixtures; Definitions, requirements, conformity, marking and labeling.  Construction Sector Specialization Committee.

Tuutti, K. (1982). Corrosion of steel in concrete. CBI Swedish Cement and Concrete Research Institute, Stockholm, 100, 159.

Virginia Department of Transportation, USA, (2007). I-295 Repaving and Repairs – Recently Completed Projects, VDOT.

Wang, S., and Li, V. C. (2006). High early strength engineered cementitious composites. *ACI Materials Journal*, **103** (2) 97-105.

Weimann, M. B. and Li, V. C. (2003). Hygral behavior of engineered cementitious composites (ECC). *International Journal for Restoration of Buildings and Monuments*, **9** (5) 513-534.

Whiting, D. and Nagi, M. (1994). Strength and durability of rapid highway repair concretes. *Concrete International*, **16** (9) 36-41.

Yang Y., Gao X., Deng H., Yu P. and Yao Y. (2010). Effects of water/binder ratio on the properties of engineered cementitious composites. *Journal of Wuhan University Technology – Mater. Sci. Ed.,* **25** (2) 298–302.

Zhang J. and Li, V.C. (2002). Monotonic and fatigue performance in bending of fiber reinforced engineered cementitious composite in overlay system. *Cement and Concrete Research*, **32** (3) 415-423.